From trace to trace maker: Oligocene–Miocene coprolites of southern Poland and their potential producers

Tomasz Brachaniec Corresp., 1 , **Dorota Środek** [1] , **Mateusz Salamon** [1] , **Michał Bugajski** [2] , **Piotr Duda** [3] , **Adam Danielak** [4] , **Magdalena Janiszewska** [4] , **Grzegorz Sadlok** [1] , **Wojciech Kuśnierczyk** [2]

[1] Department of Natural Sciences, University of Silesia, Sosnowiec, Poland

[2] Fossil Amateur Club "Inkluzja", Łódź, Poland

[3] Faculty of Science and Technology, University of Silesia, Sosnowiec, Poland

[4] Municipal Zoological Garden in Łódź, Łódź, Poland

Corresponding Author: Tomasz Brachaniec
Email address: tomasz.brachaniec@us.edu.pl

In this paper we describe coprolites from deep-marine Oligocene sediments, shallow- and deep-marine Miocene deposits, as well as Miocene continental environments in southern and central Poland. The Oligocene coprolites are classified into five morphotypes: (1) sinusoidal, (2) straight to moderately curved, (3) regular forms with macroscopically visible vertebrate remains, (4) S-shaped, and (5) oval. Sinusoidal coprolites, previously interpreted as originating from predatory fish (e.g., *Palimphyes*, *Oligophus*, and indeterminate taxa), are reinterpreted here, based on actualistic observations, as crustacean (crab) feces. Morphotypes (2)–(4) are attributed to fish, while the oval type (5) is tentatively linked to columbid-like birds, although alternative producers cannot be excluded. Miocene deep-sea coprolites are represented by relatively long, complex fecal masses composed of constricted strings, suggesting holothurians or cephalopods as potential producers. Elongated Miocene coprolites from shallow-water environments are likely to have been produced by teleost fish - most likely Sparidae - or by sharks. However, other vertebrates, including toothed and toothless cetaceans and porpoises, cannot be ruled out. The terrestial Miocene specimens include ferruginous masses with excrement-like morphologies, which, despite some controversy, are interpreted as coprolites likely produced by snakes. Another coprolite group comprises phosphatic, elongated specimens with a prominent pointed end, likely formed during anal contraction at the end of defecation. These are attributed to small mammals such as Sciuridae and/or Chiropteridae. Overall, these data provide new insights into the diversity of post-Mesozoic coprolites and refine our understanding of their producers and associated ecosystems in Central Europe.

From Trace to Trace Maker: Oligocene–Miocene Coprolites of Southern Poland and Their Potential Producers

Tomasz Brachaniec[1*], Dorota Środek[1], Mateusz Salamon[1], Michał Bugajski[2], Piotr Duda[3], Adam Danielak[4], Magdalena Janiszewska[4], Grzegorz Sadlok[1], Wojciech Kuśnierczyk[2]

[1]University of Silesia in Katowice, Faculty of Natural Sciences, Sosnowiec, Poland

[2]Fossil Amateur Club "Inkluzja", Łódź, Poland

[3]University of Silesia in Katowice, Faculty of Science and Technology, Sosnowiec, Poland

[4]Municipal Zoological Garden in Łódź [Polish limited liability company], Łódź, Poland

*corresponding author – tomasz.brachaniec@us.edu.pl

Abstract

In this paper we describe coprolites from deep-marine Oligocene sediments, shallow- and deep-marine Miocene deposits, as well as Miocene continental environments in southern and central Poland. The Oligocene coprolites are classified into five morphotypes: (1) sinusoidal, (2) straight to moderately curved, (3) regular forms with macroscopically visible vertebrate remains, (4) S-shaped, and (5) oval. Sinusoidal coprolites, previously interpreted as originating from predatory fish (e.g., *Palimphyes*, *Oligophus*, and indeterminate taxa), are reinterpreted here, based on actualistic observations, as crustacean (crab) feces. Morphotypes (2)–(4) are attributed to fish, while the oval type (5) is tentatively linked to columbid-like birds, although alternative producers cannot be excluded. Miocene deep-sea coprolites are represented by relatively long, complex fecal masses composed of constricted strings, suggesting holothurians or cephalopods as potential producers. Elongated Miocene coprolites from shallow-water environments are likely to have been produced by teleost fish - most likely Sparidae - or by sharks. However, other vertebrates, including toothed and toothless cetaceans and porpoises, cannot be ruled out. The terrestial Miocene specimens include ferruginous masses with excrement-like morphologies, which, despite some controversy, are interpreted as coprolites likely produced by snakes. Another coprolite group comprises phosphatic, elongated specimens with a prominent pointed end, likely formed during anal contraction at the end of defecation. These are attributed to small mammals such as Sciuridae and/or Chiropteridae. Overall, these data provide new insights into the diversity of post-Mesozoic coprolites and refine our understanding of their producers and associated ecosystems in Central Europe.

Keywords: terrestrial and marine bromalites, coprolites, faece, Oligocene, Miocene, Poland.

Introduction

The oldest known vertebrate coprolites date back to the Ordovician (e.g., *Hunt & Lucas, 2012*). However, most published data on coprolites pertain to the Mesozoic era (e.g, *Eriksson et al., 2011; Salamon et al., 2012; Schweigert & Dietl, 2012; Brachaniec et al., 2015; Schwimmer et al., 2015; Zatoń et al., 2015; Niedźwiedzki et al., 2016; Vajda et al., 2016; Chin, Feldman & Tashman, 2017; Segesdi et al., 2017; Barrios-de Pedro et al., 2018; Barrios-de Pedro, Chin & Buscalioni, 2020; Qvarnström et al., 2019, 2024; Lukeneder et al., 2020; Rummy, Halaçlar & Chen, 2021; Román et al., 2024* and literature cited therein).

Post-Mesozoic coprolites - or objects interpreted as such - are comparatively less documented. These have been attributed to a range of producers, including giant earthworms, fish, rodents, notoungulates, hathliacinid and borhyaenoid marsupials, hyenas and/or hyaenids and barbourofelids, as well as various indeterminate carnivorans, sirenians, and crocodilians. They have been reported from scattered localities across Europe, North and South America, and Asia (e.g., *Wetmore, 1943; Amstutz, 1958; Edwards, 1976; Wilson, 1987; Richter & Baszio, 2001; Seilacher et al., 2001; Richter & Wedmann, 2005; Dvořák et al., 2010; Godfrey & Smith, 2010;*

Peñalver & Gaudant, 2010; Pesquero et al., 2011; Stringer & King, 2012; Hunt & Lucas, 2014; Dentzien-Dias et al., 2018; Wang et al., 2018; Collareta et al., 2019; Kapur et al., 2019; Tomassini et al., 2019; Abella et al., 2021; Gross et al., 2023; Román et al., 2024). A comprehensive overview of numerous Quaternary coprolites was provided by *Hunt & Lucas (2012)*, and *Wood & Wilmshurst (2014, 2016), Tolar & Galik (2019), Agliano et al.(2024)*, and *Cambronero & García (2024)*; for review see also *Gurjãoet al. (2024)* and literature cited therein.

The only marine coprolites from post-Mesozoic sediments of Poland were thoroughly described and illustrated by *Bajdek & Bieńkowska-Wasiluk (2020)*, based on material from the Oligocene (Rupelian) of southeastern Poland. These authors documented sixteen coprolites from two localities within deep-water sediments of the Menilite Formation - an interval renowned for its spectacular fossil fish assemblages (e.g., *Bieńkowska, 2004; Kotlarczyk et al., 2006; Bieńkowska-Wasiluk, 2010*). *Bajdek & Bieńkowska-Wasiluk (2020)* concluded that the elongated, linear, often strongly sinuous, and occasionally tear-shaped coprolites they described (see table 1 and fig. 2 in *Bajdek & Bieńkowska-Wasiluk, 2020*) were most likely produced by carnivorous teleost fish.

Brachaniec et al. (2022) described 29 lacustrine, excrement-shaped ferruginous masses - referred to as "alleged" coprolites - from the Miocene (Burdigalian) deposits of the Turów lignite mine in southwestern Poland. The latter authors suggested that one of the identified morphotypes, i.e., sausage-shaped (see fig. 2A, B in *Brachaniec et al., 2022*), was likely produced by a testudinoid turtle, supported by the discovery of a shell fragment at the site. The second morphotype comprised rounded to oval-shaped fecal forms (see fig. 2E–G in *Brachaniec et al., 2022*), which were interpreted as having been produced by snakes, whose remains are abundant in the surrounding area. However, the involvement of other potential producers, such as lizards or crocodiles, could not be ruled out. Finally, *Brachaniec et al. (2022)* emphasized that although less likely, abiotic processes might also have contributed to the formation of these structures.

The aim of this study is to describe and systematically analyze numerous coprolites originating from both lacustrine and marine environments in Poland. The marine settings are represented by Oligocene and Miocene sediments from thirteen localities in southeastern Poland, while the studied lacustrine deposits are Miocene in age and come from southwestern, southern, southeastern, and central parts of Poland (*Figure 1*). The coprolites have been categorized into distinct morphotypes. Their mineralogical composition, associated fossil inclusions, palaeoecological context, and the broader palaeobiological significance of the findings are discussed in detail.

Geological setting

The field works were carried out in five areas located in southern and central Poland (see *Figure 1*).

Figure 1 around here

Kleszczów Graben area

The Kleszczów Graben is located in central Poland in Łódz Voivodeship; the graben is over 80 km long and up to 3 km wide structure ('B' on *Figure 1A*). It is the deepest tectonic depression in the Polish Lowlands as it exceeds 550 mbelow sea level in depth (*Widera, Klęsk & Urbański, 2024*). Its bedrock is formed by Permian salts and carbonates of Jurassic to Cretaceous age (e.g., *Olchowy, Krajewski & Felisiak, 2019*). The tectonic development of the graben began in Cenozoic (Paleocene) and its in-filling sediments experienced three main phases of deformation, including Valachian stage, Bełchatów stage and "upper" stage with galcitectonics (*Krzyszkowski, 1989*) and Rupelian (early Oligocene). The palaeotectonic evolution of this graben accelerated following the late Oligocene (Chattian) regional uplift. The lowermost Miocene sediments are siliciclastics consisting of sands, muds, clays, and thin layers of lignite (*Czarnecki, Frankowski & Kuszneruk, 1992*). A coal complex of lignite follows these lowermost siliciclastics of Miocene and comprises lenses of non-coal sediments and rocks, including sands, clays, lacustrine chalk, flints, sandstones, and paratonsteins (tuff horizons; *Widera, Klęsk & Urbański, 2024*). The middle Miocene succession ends with clay-coal and clay-sand complexes as seen in the Bełchatów section - these complexes have total thicknesses of up to 100–150 m (*Widera, Klęsk & Urbański, 2024*) and provide fossil plant remains and coprolites described herein.

Southern Poland (southern edge of the Holy Cross Mountains)

Miocene sediments exposed in the southern edge of the Holy Cross Mountains are located in the marginal, northern part of the Carpathian Foredeep ('C' on *Figure 1A*). This area was located in the northern part of central Paratethysin the Miocene (*Salamon et al., 2024*). The coastal and shallow-marine sediments of the area formed in an environment of moderate environmental energies (*Studencki, 1999*). Occasionally, the sediments were influenced by storms, which resulted in formation of bivalve accumulationswith numerous other fossils (*Bałuk & Radwański, 1977; Gutowski, 1984*). Abundant, large foraminifers (*Amphistegina* and *Heterostegina*) are typical for these shallow marine early Badenian Paratethys deposits. No structures indicative of linear currents have been observed, which might bean indication of high turbulence waters during the storms. One coprolite specimen comes from the so-called *Heterostegina* Sands of the Pińczów Formation of Gołuchów locality.

Lithified lower Kimmeridgian oolitic-bioclastic limestones are exposed at the Gołuchów site and fine-grained red-algal sandy limestones with isolated pebbles of the same Kimmeridgian oolitic limestones cover them. Above, fine detrital sands and poorly lithified marly sandstones are exposed. They are attributed to *Heterostegina* Sands – sediments with common foraminifers, molluscs, bryozoans, serpulids, echinoderms, and teeth of fish (*Salamon et al., 2024*) that provided the single coprolite specimen documented in this paper.

South-western Poland (Turów area)

The Turów lignite mine ('D' on *Figure 1A*) is located in the south-western part of the Lower Silesia Voivodeship (south-western Poland). It covers former village of Turów (near Bogatynia), in the central part of the mesoregion Żytawa-Zgorzelec Depression located between the state borders of Poland, Czechia and Germany. The thickness of the sediments exposed in the Turów profile is about 250 m. These sediments comprise seven lithostratigraphic units of sedimentary rocks. Most of those units are dominated by clays and/or muds with only minor intercalations of coarser facies, like sands or gravel-bearing sands (*Kasiński et al., 2015*). The oldest Cenozoic sediments of the sedimentary succession exposed herein are Oligocene sediments (Egger age), forming the lower and middle part of the Turoszów Formation (*Kasiński et al., 2015*). There are coal seams in the middle part of the profile. These seams belong to the Opolno and the Biedrzychowice Formations, which are the primary deposits exploited by the Turów mine. The coprolites described in the current study have been collected from the upper part of the Biedrzychowice Formation (Karpatian, Burdigalian; comp. *Brachaniec et al., 2022*). The youngest sediments are of the Gozdnica Formation and Pleistocene till of glacial origin. These units are, contrary to the older ones, dominated by sands and gravels (*Kasiński et al., 2015*).

South-eastern Poland (Roztocze)

The Roztocze is a geographical region in south-eastern Poland located in the Lubelskie and partly in the Podkarpackie Voivodeships. It connects the Lublin Upland with Podolia in Ukraine ('E' on *Figure 1A*). Miocene sediments of the Roztocze are dated as Badenian and Sarmatian (*Wysocka, Jasionowski & Peryt, 2007*). Although these are marine formations, determining their exact age is challenging due to the peculiarities of the depositional environment and the complex connections between the Pre-Carpathian foredeep basin and the Central and Eastern Paratethys. The use of separate lithostratigraphic schemes by Polish and Ukrainian geologists for cross-border strata further complicates age determinations (*Bogucki et al., 1998*). The investigated Miocene sediments represent diversified shallow-marine and shoreface facies: quartz sands dominate and are overlain by pelitic limestones in the lower part, and quartz-rodoid sands, organodetritic limestones, reef-type organodetritic limestones, shells, marls and serpulid-microbialitic limestones (*Musiał, 1987; Jasionowski, 1997*). Current field investigations focused on four sites (Brusno, Huta Różaniecka, Józefów, and Żelebsko; for details see e.g., *Wysocka, Jasionowski & Peryt, 2007*). Coprolites were found in Sarmatian calcarenites with spheroidal bodies of serpulid-microbial limestones at the Żelebsko site.

South-eastern Poland (Menilite-Krosno Series of the Outer Carpathians)

The Menilite-Krosno Series of the Outer Carpathians is located in southeastern Poland in the Subcarpathian Voivodeship ('E' on *Figure 1F*). At the Eocene–Oligocene boundary, tectonic activity and eustatic drop of sea level resulted in restriction of contact between sedimentary sub-basin of the Menilite-Krosno Series of the Outer Carpathians (part of the central Paratethys) and larger basin of the eastern Paratethys and ofthe Mediterranean domain (*Popov et al., 2002*). The Menilite-Krosno Series of Oligocene (Rupelian and Chattian) and Miocene (Aquitanian and

Burdigalian) comprise bituminous marlstones, cherts, shales, and sandstones with common fish fossils (e.g., *Bieńkowska-Wasiluk, 2010*). The series is a result of the activity of submarine fans, bottom currents, and deposition from low concentration turbidity currents as well as pelagic sedimentation and blooms of coccolithophores (*Kotlarczyk et al., 2006*). Current fieldworks focused on 24 sites of several hundred listed by *Kotlarczyk et al. (2006)* (*Table 1, Figure 1*), which represent both Oligocene and Miocene sediments. The studied coprolites were found in nine of the selected sites (Oligocene: Kąkolówka I, Kąkolówka II, Wola Czudecka, Futoma, Jamna Dolna, Rudawka Rymanowska, Równe, Wujskie, and Jasienica Rosielna; Miocene: Temeszów and Brzuska; for detailed geology and lithology of these localities see *Kotlarczyk et al., 2006*).

Materials and methods

Collected coprolites are housed in Sosnowiec (Poland) at the Institute of Earth Sciences, Faculty of Natural Sciences of the University of Silesia in Katowice, Poland (hereafter: IES), and catalogued under registration numbers GIUS 10–3796/O/1–300 (for Oligocene) and GIUS 10–3796/M/1–34 (for Miocene). A detailed specimen lists and descriptions are provided in *Tables 1* and *2*. Fossil fishes from *Figures 10, 13* also have been catalogued as GIUS 10–3796/O/F1–4, GIUS 10–3796V; these specimens are also housed in the IES. Fossil specimens of potential producers illustrated in *Figures 7–9, 11, 12* are from the Museum of Fossils and Minerals, Dubiecko, Poland and have catalog numbers starting with acronyms Kr., MSMD, ROJ, RORR, Ma, ROL, ROJR, ROU, ROM.

Tables 1 and 2 around here

There have been eighteen (18) coprolites studied from the Kleszczów Graben area (continental Miocene; GIUS 10–3796/M/1–5, 6, 6(1), 6(2), 6(3), 6(4), 6(5), 7–12) and five (5) of those specimens have been selected for detailed investigation in thin sections (GIUS 10–3796/M/1, 2, 6,7,11). Turów area (continental Miocene) provided eighteen (18) more specimens (GIUS 10–3796/M/14–31), and three (3) of those have been subjected to further examination in thin sections (GIUS 10–3796/M/17, 20, 27). The single specimen (GIUS 10–3796/M/13) collected from the southern edge of the Holy Cross Mountains (marine Miocene), and another one from Roztocze area (GIUS 10–3796/M/32), have been also selected for thin section analyses. There were 302 coprolites from the Menilite-Krosno Series of the Outer Carpathians (marine Oligocene and Miocene; GIUS 10–3796/O/1–300, GIUS 10–3796/M/33,34), and fifty (50) of those have been designated for detailed further analyses in thin sections (GIUS 10–3796/O/1–47, GIUS 10–3796/O/107, GIUS 10–3796/O/294, GIUS 10–3796/O/300, GIUS 10–3796/M/33,34).
Nearly all specimens were macroscopically documented in situ through field photography during field investigations. An exception was the group of elongated specimens with a distinct, prominently pointed end [(*Figure 3M*; GIUS 10–3796/M/6, 6(1), 6(2), 6(3), 6(4), 6(5)]. These were recovered by washing clay samples from the Kleszczów Graben area. Two samples were processed, weighing 40 kg and 45 kg, respectively. These samples were transported to the

laboratory in Sosnowiec (Poland) belonging to the IES. The samples were washed using running hot tap water, screened on a sieve column (Ø3.0, 1.0, 0.315 and 0.1 mm-mesh respectively), and finally dried at 150°C. This washed, screened and dried residue was observed under a Leica WildM10 microscope in search for vertebrate microremains.

The coprolites described in this article have been futher investigated with a number of different analytical tools. The methodological details are presented below.

Optical microscopy and thin-sectioning

Optical observations of thin sections have been carried out using Leica SZ-630T dissecting microscope and Nikon Eclipse E100 light microscopy, while the microphotographs have been collected using Olympus BX51 – a polarizing microscope equipped with an Olympus SC30 camera and a halogen light source (analyses conducted at the IES).

Thin sections were made in the Grindery at the IES. Specimens were embedded in Araldite epoxy resin, sectioned, mounted on the microscope slides and polished with silicon carbide andaluminum oxide powders to about 30 µm thick.

Scanning electron microscopy

The chemical composition of the coprolite matrix and embedded microfossils have been examined using the desktop scanning electron microscope (SEM) Phenom XL (Phenom World, Thermo Fisher Scientific, Netherlands), equipped with a fully integrated energy-dispersive X-ray spectroscopy (EDS) detector and secondary electron detector (SED), located at the IES. The observations were conducted under low-vacuum conditions with an accelerating voltage of 15 kV. Samples were not coated.

Microtomography

One representative specimen from each identified morphotype was selected for virtual sectioning (specimens no. GIUS 10–3796/O/2, GIUS 10–3796/O/9, GIUS 10–3796/O/18, GIUS 10–3796/O/21, GIUS 10–3796/O/30, GIUS 10–3796/O/111, GIUS 10–3796/M/3, GIUS 10–3796/M/6, GIUS 10–3796/M/9, GIUS 10–3796/M/12, GIUS 10–3796/M/13, GIUS 10–3796/M/18, GIUS 10–3796/M/21, GIUS 10–3796/M/32, GIUS 10–3796/M/34).

In microtomographic studies, the flat shape of the samples in the form of a disc makes it difficult to optimally position them in relation to the radiation source and the detector. Precise positioning is also required so that the X-ray beam penetrates the entire thickness of the sample without losing focus. Incorrect positioning leads to image distortions (artefacts) caused by differences in the thickness of the x-rayed layers and to difficulties in 3D reconstruction due to the limited number of projection angles. Due to these difficulties some of the samples had to be cut using a mini-grinder. The form of columns facilitates imaging using an X-ray scanner.

Microtomographic studies were carried out in the Laboratory of Computed Microtomography of the Institute of Biomedical Engineering of the University of Silesia in Katowice. The samples were scanned at voltage parameters of 160 kV and current of 50 µA, 100 µA with resolutions of 8 µm, 10 µm and 25 µm. Each projection with a resolution of 2024x2024 pixels consisted of three repetitions with an exposure time of 500 ms. The scanning time of the coprolites was about one hour during which 2100 x-rays were taken.

The images after reconstruction were processed using Volume Graphics®VGSTUDIO Max software, where image normalization and appropriate positioning and geometric measurements were performed. Visualization, animations and detailed analysis were performed using the Volume Graphics®myVGL viewer.

Observations of extant excrements

For comparative observations, more than 400 feces from contemporary animals were collected over a period of six months. The collected excrements belonged to invertebrates (crabs) and vertebrates (fish, reptiles, birds, and mammals). They were all collected in the animals' natural habitat in the Municipal Zoological Garden in Łódź, Poland. For comparative purposes, we also used archived data on the feces of fish, amphibians, reptiles, birds, and mammals, which were collected in 2021 at the Silesian Zoological Garden in Chorzów, Poland (for details see *Brachaniec et al., 2022*). External and internal features of the fecal masses were analyzed. Particular attention was given to those clades that have representatives in the Oligocene and Miocene sediments of Poland and neighbouring areas, and could therefore have been among the producers responsible for the studied coprolites.

Results

Coprolite morphology

A total of 339 coprolites were collected: 300 from Oligocene and 39 from Miocene sediments (for details see *Table 1* and *2*). Six different morphotypes were distinguished, characterized by different shapes and sizes (sinusoidal; elongated; straight,curved; irregular; S-shaped; and oval); for details see *Tables 1–4*, *Figures 2–3*.

Tables 3 and 4 around here

The colours of coprolites varied, even within the same morphotype and age group. Oligocene (M-KS) sinusoidal forms were most often black (51%) and brown (49%). Black (43%), brown (37%), grey (19%), and red (2%) specimens were found also among elongated Oligocene coprolites.The oval and the regular ones were grey (77%), red (21%), and pastel (2%) in colour. The S-shaped coprolites were black (60%), brown (30%), and red (105). Finally, the curved forms were red (70%), brown (25%), and grey (5%).

In the case of continental Miocene specimens (Turów area), their colours varied from pale orange, through greenish red, to burgundy-colored. The ferruginous specimens from Kleszczów Graben were celadon, brown-blue, and locally red. Six specimens were light pastel to light brown. Specimens from the marine Miocene of Roztocze area and Gołuchów quarry (the edge of the Holy Cross Mountains) were light orange and light brown, respectively.

Figures 2 and 3 around here

Microtomographic, optical and SEM microscopy studies

Microtomographic studies of terrestrial Miocene coprolites did not reveal any well visible internal structures (Movie S1) that could constitute some undigested food remains [(GIUS 10–3796/M/3, GIUS 10–3796/M/6, GIUS 10–3796/M/9, GIUS 10–3796/M/12) – Kleszczów Graben area; (GIUS 10–3796/M/18, GIUS 10–3796/M/21) – Turów area)]. The same is true for three specimens from marine Miocene environments [(GIUS 10–3796/M/13) – Gołuchów quarry in southern edge of the Holy Cross Mountains; (GIUS 10–3796/M/32) – Żelebsko in Roztocze area; (GIUS 10–3796/M/34) – Brzuska locality in Menilite-Krosno Series of the Outer Carpathians]. However, the specimens from Oligocene marine sediments differed in this respect [(GIUS 10–3796/O/2, GIUS 10–3796/O/18, GIUS 10–3796/O/9, GIUS 10–3796/O/21, GIUS 10–3796/O/30, GIUS 10–3796/O/111) – in all specimens from Menilite-Krosno Series of the Outer Carpathians, some undigested food remains were observed, and these food item remnants include mostly remains of fish (bones, scales and teeth; see *Supplementary movie 1*).

Thin sections made ~~fromcontinental~~ Miocene coprolites were analyzed in transmitted and reflected light. Dark, nearly opaque matrix can be seen in the specimens from Kleszczów Graben area (GIUS 10–3796/M/1, GIUS 10–3796/M/2, GIUS 10–3796/M/7, GIUS 10–3796/M/11) and from Turów area (GIUS 10–3796/M/17, GIUS 10–3796/M/20, GIUS 10–3796/M/27). The mineral matrix is homogeneous and some elongated structures can be observed within it. These elonged features have arcuate shapes in some cases and they appear to be light-reduction areas in reflected light whereas the surrounding matrix was oxidized. The dark (rusty, brown to almost black), slightly transparent colour of the matrix suggests an iron-rich mineral(s) that formed the matrix. No other distinguishable microdebris were observed. A bright matrix can be observed ~~inone specimenwhen~~ seen under transmitted light [(GIUS 10–3796/M/6) – Kleszczów Graben area]. No biogenic remains were observed in this case, only some indeterminate mineral structures. Similar results of thin section analyses were obtained from the specimenscollected from the southern edge of the Holy Cross Mountains (marine Miocene; (GIUS 10–3796/M/13) and Roztocze area (GIUS 10–3796/M/32).

A bright and opaque matrix can be observed in thin sections made from the marine Oligocene and Miocene coprolites of the Menilite-Krosno Series of the Outer Carpathians (GIUS 10–3796/O/1–47, GIUS 10–3796/O/107, GIUS 10–3796/O/294, GIUS 10–3796/O/300, GIUS 10–3796/M/33, 34). The matrix is homogeneous in most of the analyzed samples, however in same cases small structures with angular edges can be noted. Numerous fish remains can be observed embedded within the matrix, and these remains, after further examination under SEM (*Figures 4, 5*), have been found to represent fish bones, scales and teeth. There were no fossil remains of fish or other organisms observed in thin sections made from specimens: GIUS 10–3796/M/33 and GIUS 10–3796/M/34 (Miocene of the Menilite-Krosno Series of the Outer Carpathians).

Movie S1 around here

Figure 4 around here

Mineralogical and structural analyses

The chemical composition (SEM) analysis of coprolite no. GIUS 10–3796/M/33 revealed that the coprolite matrix is highly porous and consists of microcrystalline fluorapatite, which occurs in small (about 0.5–4 µm in diameter) thin-walled vesicles. These forms are considered mineral pseudomorphs of organic structures in the original feces (*Hollocher et al., 2010*). Some researchers suggest that this specific structure is associated with spherical bacteria, such as *Enterococcus faecalis*, and other common cocci found in feces (*Hollocher et al., 2010*). It has also been shown that under natural conditions and in laboratory experiments, bacteria, and even their phosphatases, can promote the precipitation of microcrystalline apatite (*Hirschler, Lucas & Hubert, 1990; Lucas & Prévôt, 1991; Jehl & Rougerie, 1995*), which suggests that the fecal bacteria themselves may have been involved in the apatite mineralization process (*Hollocher et al., 2010*). There are fragments embedded within the porous matrix that have lower porosity and are composed of fluorapatite of clearly organic origin (*Figures 4,5*). These microfossils most likely represent bone fragments, teeth, and remnants of plant tissues. Additionally, the matrix contained mineral grains such as quartz and zircon, as well as crystals that had formed within the voids of the coprolites, including calcite and framboidal pyrite. The only coprolite with a different chemical composition was ~~onespecimen~~ from Turów. This specimen had also porous matrix structure but it consists of iron oxides and hydroxides. No microfossils were found within it.

Figure 5 around here

Contemporary comparative studies

The visual comparison made it possible to exclude modern feces that differed significantly from the analyzed coprolites in terms of size and shape. These feces samples were not taken into account in further analyses. The subsequent observations were based on a morphological comparison between the selected recent feces and the studied coprolites. Surprisingly, crabs (*Coenobita brevimanus*) were observed to produce fecal masses of sinusoidal morphology (*Figure 6J*) similar to coprolites described by us from the Oligocene (see e.g., *Figures 2C-E, 3B*). Nearly identical sinusoidal feces (see *Figure 6K*) were produced by another crab (flying crab, *Liocarcincus holsatus*), which is closely related to fossil representatives of *Liocarcinus* – a taxon commonly found in the Menilite-Krosno Series of the Outer Carpathians. So far, this type of coprolite morphology has been attributed to predatory fishes (e.g., *Bajdek & Bieńkowska-Wasiluk, 2020*). However, despite the examination of numerous faces produced by extant fish taxa (a total of 30 species belonging to Scombriformes and Gadiformes), no corresponding sinusoidal morphology has been observed in the fecal remains of any of these taxa. The observed recent feces of studied fish taxa were dominated by masses with morphologies resembling coprolites' morphologies classified ~~intostraight~~, curved, and S-shaped categories (see *Figure*

6N). These fish-produced fecal masses comprised various remains of other, presumably consumed fish individuals (bones, scales, teeth). Noteworthy, the studied coprolites with similar morphologies also contain fossil fish remnants.

Current observations show that barracudas produce more or less regular feces, sometimes slightly tapering on one side (comp. *Figure 6I*). There is a similar morphological type in the studied sample of Oligocene coprolites (more or less regular with macroscopically visible vertebrate remains; *Figures 2O, 3C*). It is likely, based on morphologic and size criteria, that this fossil coprolite specimen was also produced bybarracuda (*Sphyraena*).

Oval and relatively large coprolites from the Oligocene marine sediments (*Figure 2U*) do not contain any faunal remains. Their shape and size resemble the fecal masses produced by members of the bird family Columbidae (*Figure 6H*). Noteworthy, fossil remains of these birds have been documented in the Menilite-Krosno Series of the Outer Carpathians (*Bocheński, Tomek & Świdnicka, 2010*).

Deep-sea coprolites documented from the Miocene deposits are represented by relatively long and complex faecal masses consisting of string with frequent constrictions (*Figure 3D*). These fossil specimenshave morphology most closely resembling feaces of holothurians (*Holothuria* sp.; *Figure 6L*) and cephalopods (*Nautilus pompilius*; *Figure 6M*).

The last type of bromalites compared with recent fecal masses consists of phosphatic specimens recovered from continental Miocene strata. These coprolites are elongated and exhibit a characteristic, prominently pointed end, likely formed as the anus contracted to close and sever the expelled fecal mass (*Figure 3M*). Among vertebrates inhabiting the present-day terrestial environments of central Poland, the feces of Sciuridae and Chiropteridae are most comparable to the fossil specimens, as they are similarly small and display a distinct pointed termination at one end (*Figures 6D, E*).

Figure 6 around here

Discussion

Oligocene marine coprolites

Majority of the currently documented coprolites come from the Oligocene sediments of the Menilite-Krosno Series of the Outer Carpathians in southern Poland (for details see *Table 1*). *Bajdek & Bieńkowska-Wasiluk (2020)* argued that the high abundance of mesobathypelagic fish remains documented in these sediments may point to a well-oxygenated deep-marine environment (likely exceeding 500 m in some places). *Kotlarczyk et al. (2006)* concluded that the basin depth in this area could have been even greater, locally exceeding 2,000 m. The coprolites from these deep marine facies were classified into five morphotypes. The first type, characterized by a sinusoidal shape, was previously recorded from Oligocene strata in southern Poland (*Bajdek & Bieńkowska-Wasiluk, 2020*). These authors concluded that these coprolites were produced by fish predators, mainly representatives of *Palimphyes*, *Oligophus*, and an indeterminate gadiform. However, current experimental studies suggest that similar faecal morphologies could also be associated with invertebrates, such as crabs, whose fossils are relatively common in the Menilite-Krosno Series (*Jerzmańska, 1967; Bieńkowska-Wasiluk, 2010*; *Figure 7*). Although *Bajdek & Bieńkowska-Wasiluk (2020)* considered crabs as potential producers, they ultimately ruled them out, reasoning that the crabs known from these strata were too small to produce long, sinusoidal coprolites. Noteworthy, the lengths of faecal strings may approach the body lengths of their producers. Furthermore, when estimating producer size, the total faecal mass or the diameter of the coprolite may serve as more reliable indicators of the producer's body size or anus size, respectively, than the length of faecal strings (see *Donovan, 1994*). Our experimental studies demonstrate that crabs are capable of producing long faecal strings with sinusoidal morphologies comparable to those observed in the studied fossil coprolites (cf. *Figure 2A-E* and *Figure 6K*).

We suggest that the three successive morphotypes, i.e., straight, curved with macroscopically visible vertebrate remains, and S-shaped, were produced by fish (see *Figures 8-11*). Morphologically similar non-spiral coprolites (e.g., *Figure 2F–J*) are known from the Eocene deposits of the Green River Formation (*Edwards, 1976*), the Coldwater Beds (*Wilson, 1987*), and Messel (*Richter & Wedmann, 2005*). Rope-like (non-spiral) faecal masses are commonly produced by teleost fishes (see *Figure 6N*), representatives of which inhabited the Oligocene marine environments in southern Poland. Furthermore, our experimental studies indicate that barracudas may produce more or less regular faecal strings, sometimes terminating in a slightly tapering end (cf. *Figure 6I*). Noteworthy, *Kotlarczyk et al. (2006)* also reported the presence of barracudas in the Polish Carpathians.

Identifying the producer of the oval coprolite (*Figure 2U*) is challenging. None of the marine taxa known from the Menilite-Krosno Series sediments could be easily linked to this morphology based on current experimental results. However, the morphology and size of the coprolite resemble,to some extent, the excrements of some birds, particularly pigeons (Pigeonidae). Noteworthy, the remains of these birds have been reported from Carpathian sediments (*Bocheński, Tomek & Świdnicka, 2010*). However, before this interpretation can be further substantiated, a thorough taphonomic analysis of the preservation pathway of bird faeces in marine deposits is required. *Bocheński, Tomek & Świdnicka (2010)* also reported fossils of humming birds and some passerines from the same strata. However, the shape and size of the faeces of these taxa differ from those of the studied coprolites (*Bocheński & Bocheński, 2008; Bocheński et al., 2011*; see *Figure 6F*).

Figures 7-12 around here

Miocene marine coprolites

Four coprolites were recorded in the marine Miocene sediments (for details see *Table 4*). Two of them (GIUS 10–3796/M/13, 32; *Figure 3E, F*) come from shallow marine deposits displaying high variation of lithologies, facies, and thicknesses (Roztocze area and southern edge of the Holy Cross Mountains). There have been no predatory vertebrates documented in the Żelebsko quarry (Roztocze area) that could have been responsible for the production of the documented apatite faeces. The dominant species at the site are gastropods, bivalves, and foraminifers. However, fossil fish teeth are common in a nearby Gołuchów quarry exposing the sediments of the same age (southern edge of the Holy Cross Mountains). These fossils co-occur at the site with fossils of invertebrates, including foraminifers, molluscs, bryozoans, serpulids, echinoderms (asteroids, echinoids and stalked crinoids (*Salamon et al., 2024*). Most of the fish teeth at the site represent teleost fish (above 70% collected specimens; *Salamon et al., 2024*). They belonged to the family Sparidae. There have been also shark teeth, but those were less numerous, and belonged mainly to the Odontaspididae family, including *Carcharias acutissima* and *Araloselachus* cf. *vorax*. *Salamon et al. (2024)* also documented shark teeth (68% of all specimens), belonging to at least four families, in the nearby locality of Zygmuntów near Książ Wielki (see fig. 2 in *Salamon et al., 2024*). Fossil teeth assigned to *Otodus megalodon*, *Cosmopolitodus hastalis*, *Isurus*, and *Galeocerdo* were found thereas well; myliobatoid teeth were also occasionally noted (*Aetobatus*). According to *Salamon et al. (2024)* teleost fish teeth and tooth plates constitute 24% of the collected teeth specimens, and are represented only by Sparidae. A logical step in the challenging task of producer identification would be to seek potential candidates among predatory taxa represented by fossil teeth. The identification, however, is further complicated by the absence of recognizable faunal remains within the coprolite matrix. The list of potential producer candidates can be even longer as other predatory vertebrates (toothed and toothless cetaceans, porpoises) have been recognized in the northern (Polish) part of Miocene Paratethys (*Czyżewska & Radwański, 1991* and literature cited therein). These mammals cannot be excluded as the potential producers of coprolites from Żelebsko and Gołuchów. *Bałuk (1977)* documented numerous remains of cephalopods within the Korytnica Clays of the southern margin of the Holy Cross Mountains. However, the morphology of fossil and extent faeces assignable to these invertebrates (comp. *Knaust & Hoffmann, 2020*, and literature cited therein) differ from the coprolites from Żelebsko and Gołuchów.

Two coprolites (GIUS 10–3796/M/33, 34; *Figure 3D*) have been collected from the Menilite-Krosno Series (The Outer Carpathians, Poland) – strata representing marine environment, probably exceeding 500 m depth (*Bajdek & Bieńkowska-Wasiluk, 2020*). These are relatively long and complex faecal masses, each consisting of string with frequent constrictions. These features make them similar to the faeces of extent sea cucumbers and cephalopods (see fig. 6, 7 in *Knaust & Hoffmann, 2020*; *Figure 6L, M*). However, holothurians have not been described so far from the Menilite-Krosno Series, and only a single cephalopod specimen has been described from the strata (*Świdnicka, 2007*). Therefore, identification of potential producers must remain speculative as body fossil record is missing or not sufficient. No fossil remains of consumed taxa have been found in the faecal matrix, hindering the producer identification even more problematic.

Miocene continental coprolites

There are excrement-like masses (pellets) that are frequently recorded from various clayey sediments (for review see *Brachaniec et al., 2022*). However, some researchers rule out zoological origin of those pellets, despite their superficial similarity to faecal masses.The main characteristics cited against the biological origins of those, are: their ferruginous composition, variation in size, lack of internal inclusions, and scarcity of associated (embedded) vertebrate remains (e.g., *Roberts, 1958; Dake, 1960; Danner, 1994, 1997; Spencer & Tuttle, 1980; Love & Boyd, 1991; Spencer, 1993, 1997; Hardie, 1994; Mustoe, 2001*).

Several hypotheses have been proposed to explain the origin of these problematic masses, including: co-seismic lique faction, sediment intrusion into hollow logs or between plant stems, expulsion of sediment under gravitational pressure, and siderite extrusion driven by methanogenesis (*Spencer & Tuttle, 1980; Love & Boyd, 1991; Spencer, 1993; Peterson & Madin, 1997; Mustoe, 2001*). However, there have been also a few authors who interpreted these masses as biological in nature, either as fossil faeces (coprolites), cololites, or evisceralites (*Amstutz, 1958; Broughton, Simpson & Whitaker, 1977; Broughton, Simpson & Whitaker, 1978; Seilacher et al., 2001; Broughton, 2017; Brachaniec et al., 2022*). Recently, *Brachaniec et al. (2022)* presented a detailed study of excrement-shaped ferruginous masses from the Miocene strata of Poland (Turów, south-west Poland). The authors described two coprolite morphotypes: the first includes small, sausage-shaped specimens, while the second comprises larger, more rounded to oval, massive specimens with a rough surface, sometimes exhibiting a prominent pointed end covered by a striated pattern, interpreted as a morphology resulting from anal contraction during the cutting off of the expelled portion of the faecal mass.The latter authors combined their palaeontological and mineralogical analytical results with experimental data and concluded that these structures may represent "true" coprolites, which were likely produced by reptiles [smaller morphotype – by tortoises (Testudinoidea)] and larger one – by snakes (Serpentes)]. This conclusion was supported by the morphological match between the fossil and experimental faecal masses (including fine striations), as well as by the presence of hair-like structures (or coalified inclusions) within the coprolites, which could suggest a diet including mammals.

In the current study (see Table 4) we documented thirty (30) ferruginous coprolites (GIUS 10–3796/M/1–12, 14–31). These specimens have been collected from two regions of southern Poland (the Turów area and the Kleszczów Graben area). All these coprolites are represented by one morphotype only (II morphotype sensu *Brachaniec et al., 2022*; i.e,, more rounded to oval, elongate, massive specimens with rough surface; *Figure 3G-L, N*). These coprolites comprise numerous hair-like structures, coalified inclusions, and traces of fine striations visible on the surfaces. These features make them similar to other Miocene coprolites ascribed so far to snakes (fig. 2H-M in *Brachaniec et al., 2022*). However, other producers cannot be ruled out definitively at this stage. A rich assemblages of continental tetrapod fauna have been documented from slightly older sediments (Eocene and Oligocene) of surrounding areas (north-western Bohemia and south-eastern Germany). *Brachaniec et al. (2022)* mentioned other fossil representatives, including frogs, salamanders, choristoderans, crocodiles, turtles, lizards, and snakes from these regions (for details see table 1 in *Brachaniec et al., 2022*). The same authors noted that vertebrate fossil remains are abundant in the Miocene of northern Bohemia (North

Bohemian Brown Coal Basin in Czechia), and are represented by osteichthyan fish, amphibians, reptiles, birds, and mammals, among others (for details see table 2 in *Brachaniec et al., 2022*). Rodents of Sciuridae family could be responsible for the apatite coprolites with a characteristic and prominent pointed termination, that likely formed due to contraction of anus closing to cut off the faecal mass (GIUS 10–3796/M/6, 6(1), 6(2), 6(3), 6(4), 6(5); *Figure 3M*). Such coprolites have been found in the sediments of the Kleszczów Graben area (*Garapich, 2002; Kowalski & Rzebik-Kowalska, 2002*). *Chame (2003)* studied excrements of extant mammals and illustrated small (max. length 1.5 cm) faeces, with a narrowing termination (see table 1 in *Chame, 2003*). This type of faeces was produced by Sciuridae (*Chame, 2003*). Alternatively, it is also possible that representatives of Chiropteridae produced this type of coprolites from the Kleszczów Graben – indeed their fossil remains in the strata have been documented by *Garapach (2002*; see also *Figure 13*).

The current actualistic studies show that bat (*Carollia perspicillata*) may produce elongated faeces with a characteristic prominent pointed end formed during anus closing (*Figure 6E*). The bat faeces resemble some of the studied fossil specimens (cf. *Figure 3M*). Based on the combination of morphology and size, we exclude the possibility that this type of coprolite was produced by representatives of Talpidae, Castoridae, Caviidae, or lizards, despite the presence of their fossils in the sedimentary strata of the Kleszczów Graben (*Garapich, 2002* and literature cited therein; comp. *Figure 6* and data presented in *Brachaniec et al., 2021*).

Other groups of organisms recorded from this area are malacofauna (*Stworzewicz, 1999*), fish (*Kovalchuk et al., 2019*), and crustaceans (*Dumont et al., 2020*). During fieldwork, we documented also other co-occurring fossils represented by bone elements, vertebrae, teeth, and otoliths of freshwater fish belonging to Gobioidae, Umbridae, Cyprinidae, Pleuronectoidae, Apogonidae and"*Anguilloides*" sp. (an extinct relative of an eel). However, the robust morphology (including the pointed termination) and size make representatives of these groups rather unlikely candidates for the producers of the studied ferruginous coprolites.

Figure 13 around here

Supplemental Information

A movie showing the internal structure of a selected Oligocene (Rupelian) coprolite of the Kąkolówka locality, southern Poland (specimen no. GIUS 10–3796/O/9).

ADDITIONAL INFORMATION AND DECLARATIONS

Author Contributions

Tomasz Brachaniec designed research, analyzed the data, prepared figures and/or tables, and approved the final draft.

Dorota Środek performed the mineralogical analyses, analyzed the data, prepared figures, and approved the final draft.
Mateusz Salamon conducted field works and acquired a specimen for research.
Michał Bugajski conducted field works and acquired a specimen for research.
Piotr Duda performed the microtomographic studies.
Adam Danielak performed photos of recent faeces.
Magdalena Janiszewska performed photos of recent faeces.
Grzegorz Sadlok analyzed the data and approved the final draft.
Wojciech Kuśnierczyk conducted field works and acquired a specimen for research.

Competing Interests

The authors declare that they have no competing interests.

Data availability

All data generated or analysed during this study are included in this published article. For the purpose of Open Access, the first author has applied a CC-BY public copyright licence to any Author Accepted Manuscript (AAM) version arising from this submission.

Funding

This research was funded in whole by the National Science Centre, Poland (www.ncn.gov.pl), grant no. 2023/49/B/ST10/00322 for Tomasz Brachaniec.

Acknowledgements

Journal reviewers and editor are acknowledged for improving the quality of this study. Special thanks are due to the all employees and authorities of Municipal Zoological Garden in Łódź, Poland, thanks to whom it was possible to carry out actualistic research. Authors thanks to Tomasz Janiszewski for photos of bird faeces, zoological shop “Rybka” for fish faeces, Robert Szybiak for lending some of the specimens for research, and Wojciech Krawczyński for photo documentation. Maciej Pindakiewcz and Adiel A. Klompmaker are ackowledged for otholits and crabs assignation.

References

Abella J, Martin-Perea DM, Valenciano A, Hontecillas D, Montoya P, Morales J. 2021. Coprolites in natural traps: direct evidence of bone-eating carnivorans from the Late Miocene Batallones-3 site, Madrid, Spain. *Lethaia* **54**:762-774 DOI 10.1111/let.12438.

Agliano F, Velázquez NJ, Martínez Tosto AC, Camiolo IS, Rindel DD. 2024. Camelid diet through microhistological and palynological analyses of feces and coprolites from Parque Nacional Perito Moreno, Patagonia, Argentina. *Journal of Archaeological Science: Reports* **58**:104713 DOI 10.1016/j.jasrep.2024.104713.

Amstutz G. 1958. Coprolites: a review of the literature and a study of specimens from Southern Washington. *Journal of Sedimentary Petrology* **28**:498-508 DOI 10.1306/74d7084e-2b21-11d7-8648000102c1865d.

Bajdek P, Bieńkowska-Wasiluk M. 2020. Deep-sea ecosystem revealed by teleost fish coprolites from the Oligocene of Poland. *Palaeogeography, Palaeoclimatology, Palaeoecology* **540**:109546 DOI 10.1016/j.palaeo.2019.109546.

Bałuk W. 1977. A new species of the cuttlefish from the Korytnica Clays (Middle Miocene; Holy Cross Mountains, Poland). *Acta Geologica Polonica* **27**:169-176

Bałuk W, Radwański A. 1977. Organic communities and facies development of the Korytnica Basin (Middle Miocene; Holy Cross Mountains, Central Poland). *Acta Geologica Polonica* **27**:85-123

Barrios-de Pedro S, Poyato-Ariza FJ, Moratalla JJ, Buscalioni ÁD. 2018. Exceptional coprolite association from the Early Cretaceous continental Lagerstäte of Las Hoyas, Cuenca, Spain. *PloS ONE* **13**:e0196982 DOI 10.1371/journal.pone.0196982.

Barrios-de Pedro S, Chin K, Buscalioni AD. 2020. The late Barremian ecosystem of Las Hoyas sustained by fishes and shrimps as inferred from coprofabrics. *Cretaceous Research* **110**:104409 DOI 10.1016/j.cretres.2020.104409.

Bieńkowska M. 2004. Taphonomy of ichthyofauna from an Oligocene sequence (Tylawa Limestones horizon) of the Outer Carpathians. Poland. *Geological Quarterly* **48**:181-192

Bieńkowska-Wasiluk M. 2010. Taphonomy of Oligocene teleost fishes from the Outer Carpathians of Poland. *Acta Geologica Polonica* **60**:479-533

Bocheński Z., Bocheński ZM. 2008. An Old World hummingbird from the Oligocene: a new fossil from Polish Carpathians. *Journal of Ornithology* **149**:211-216 DOI 10.1007/s10336-007-0261-y.

Bocheński ZM, Tomek T, Świdnicka E. 2010. A columbid-like avian foot from the Oligocene of Poland. *Acta Otnithologica* **45**:233-236 DOI 10.3161/000164510X551363.

Bocheński ZM, Tomek T, Bujoczek M, Wertz K. 2011. A new passerine bird from the early Oligocene of Poland. *Journal of Ornithology* **152**:1045-1053 DOI 10.1007/s10336-011-0693-2.

Bogucki A, Gerasimow L, Wołoszyn P, Wysocka A. 1998. *Budowa geologiczna Roztocza Ukraińskiego*. Przewodnik LXIX Zjazdu PTG: Lublin. 245-256

Brachaniec T, Niedźwiedzki R, Surmik D, Krzykawski T, Szopa K, Gorzelak P, Salamon MA. 2015. Coprolites of marine vertebrate predators from the Lower Triassic of southern Poland. *Palaeogeography, Palaeoclimatology, Palaeoecology* **435**:118-126 DOI 10.1016/j.palaeo.2015.06.005.

Brachaniec T, Środek D, Surmik D, Niedźwiedzki R, Georgalis GL, Płachno BJ, Duda P, Lukeneder A, Gorzelak P, Salamon MA. 2022. Comparative actualistic study hints at origins of alleged Miocene coprolites of Poland. *PeerJ* **10**:e13652 DOI 10.7717/peerj.13652.

Broughton PL. 2017. Enigmatic origin of massive late Cretaceous-to-Neogene coprolite-like deposits in North America: a novel palaeobiological alternative to inorganic morphogenesis. *Lethaia* **50**:194-216 DOI 10.1111/let.12186.

Broughton PL, Simpson F, Whitaker SH. 1977. Late Cretaceous coprolites from southern Saskatchewan: comments on excretion, plasticity and ichnological nomenclature. *Bulletin of Canadian Petroleum Geology* **25**:1097-1099

Broughton PL, Simpson F, Whitaker SH. 1978. Late Cretaceous coprolites from Western Canada. *Palaeontology* **21**:443-453

Cambronero I, García N. 2024. Does size matter? Morphological and content analysis of the coprolites from a Quaternary deposit in the IberianPeninsula. *Quaternary Environments and Humans* **2**:100009 DOI 10.1016/j.qeh.2024.100009.

Chame M. 2003. Terrestrial mammal feces: a morphometric summary and description. *Memórias do Instituto Oswaldo Cruz* **98 (Suppl. I)**:71-94 DOI 10.1590/S0074-02762003000900014.

Chin K, Feldmann RM, Tashman JN. 2017. Consumption of crustaceans by megaherbivorous dinosaurs: dietary flexibility and dinosaur life history strategies. *Scientific Reports* **7**:11163 DOI 10.1038/s41598-017-11538-w.

Collareta A, Gemelli M, Varola A, Bianucci G. 2019. Trace fossils on a trace fossil: A vertebrate-bitten vertebrate coprolite from the Miocene of Italy. *Neues Jahrbuch für Geologie und Paläontologie, Abhandlungen* **293**:117-126 DOI 10.1127/njgpa/2019/0834.

Czarnecki L, Frankowski R, Kuszneruk J. 1992. Synthetic lithostratigraphic profile of Tertiary deposits of the Bełchatów deposit. In: Lipiarski I, ed. *Geologia formacji węglonośnych Polski*. Wydawnictwo Akademii Górniczo-Hutniczej: Kraków. 18-23

Czyżewska T, Radwański A. 1991. Middle Miocene (Badenian) delphinid and phocoenid remains from the Fore-Carpathian Depression in southern Poland. *Acta Geologica Polonica* **41**:183-191

Dake HC. 1960. Washington coprolites again. *Mineralogist* **28**:2-6

Danner WR. 1994. The pseudocoprolites of Salmon Creek, Washington. University of British Columbia Department of Geological Sciences Report.

Danner WR. 1997. The pseudocoprolites of Salmon Creek, Washington.

Dentzien-Dias P, Carrillo-Briceño JD, Francischini H, Sánchez R. 2018. Paleoecological andtaphonomical aspects of the late Miocene vertebrate coprolites (Urumaco Formation) ofVenezuela. *Palaeogeography, Palaeoclimatology, Palaeoecology* **490**:590-603 DOI 10.1016/j.palaeo.2017.11.048.

Donovan SK. 1994. The palaeobiology of vertebrate coprolites. In: Donovan, SK. ed. *The Palaeobiology of Trace Fossils*. John Wiley & Sons Ltd.: Chichester. 221-239

Dumont HJ, Pociecha A, Zawisza E, Szeroczyńska K, Worobiec E, Worobiec G. 2020. Miocene cladocera from Poland. *Scientific Reports* **10**, 12107 DOI 10.1038/s41598-020-69024-9.

Dvořák Z, Mach K, Prokop J, Knor S. 2010. *Třetihorni fauna severočeské hnědouhelné pánve*. Prague: Nakladatelství Granit.

Edwards P. 1976. *Fish Coprolites from Fossil Butte, Wyoming*. Wyoming: Contributions to Geology.

Eriksson, ME, Lindgren J, Chin K, Månsby U. 2011. Coprolite morphotypes from the Upper Cretaceous of Sweden: novel views on an ancient ecosystem and implications for coprolite taphonomy. *Lethaia* **44**:455-468 DOI 10.1111/j.1502-3931.2010.00257.x.

Garapich A. 2002. An overview of Miocene rodents from Bełchatów (Poland). *Folia Zoologica* **51 (Suppl. 1)**: 59-66

Godfrey JS, Smith BJ. 2010. Shark-bitten vertebrate coprolites from the Miocene of Maryland. *Naturwissenschaften* **97**:461-467 DOI 10.1007/s00114-010-0659-x.

Gross M, Prieto J, Grímsson F, Bojar HP. 2023. Hyena and 'false' sabre-toothed cat coprolites from the late Middle Miocene of south-eastern Austria. *Historical Biology* **36**: 1903-1922 DOI 10.1080/08912963.2023.2237979.

Gurjão L, Dias O, Neto J, Iñiguez A. 2024. Coprolite diversity from the archeological site Gruta Do Gentio Ll, Unaí, Minas Gerais, Brazil. *The Holocene* **34**:1765-1774 DOI 10.1177/09596836241275019.

Gutowski J. 1984. Sedimentary environment and synecology of macrobenthic assemblages of the marly sands and red-algal limestones in the Korytnica Basin (Middle Miocene; Holy Cross Mountains, Central Poland). *Acta Geologica Polonica* **34**:323-340

Hardie JK. 1994. Dolomite and siliciclastic dikes and sills in marginal-marine Cretaceous coals of central Utah. *U.S. Geological Survey Bulletin* **2087**:1-19

Hirschler A, Lucas J, Hubert JC. 1990. Apatite genesis: A biologically induced or biologically controlled mineral formation process?. *Geomicrobiology Journal* **7**:47-56

Hollocher KT, Hollocher TC, Keith Rigby Jr.J. 2010. A Phosphatic Coprolite Lacking Diagenetic Permineralization From The Upper Cretaceous Hell Creek Formation, Northeastern Montana: Importance Of Dietary Calcium Phosphate In Preservation. *Palaios* **25**:132-140 DOI 10.2110/palo.2008.p08-132r.

Hunt AP, Lucas SG. 2012. Classification of vertebrate coprolites and related trace fossils. *New Mexico Museum of Natural History and Science Bulletin* **57**:137-146

Hunt AP, Lucas SG. 2014. Jurassic vertebrate bromalites of the western United States in the context of the global record. *Volumina Jurassica* **12**:151-158 DOI 10.5604/17313708 .1130139.

Jasionowski M. 1997. Zarys litostratygrafii osadów mioceńskich wschodniej części zapadliska przedkarpackiego. *Biuletyn Państwowego Instytutu Geologicznego* **373**:43-60

Jehl C, Rougerie F. 1995. Phosphatogenese en atolls polynesiens: La filiation mattes cyanobacteriennes-phosphorites. *Oceanologica Acta* **18**:79-93

Jerzmańska A. 1967. Crabs of the genus *Portunus* Weber from the Menilite Series of the Carpathians. (In Polish, English summmary). *Annales de la Société Géologique de Pologne* **37**:539-545

Kapur VV, Kumar K, Morthekai P, Chaddha AS. 2019. Palaeodiet of Miocene producer(s) and depositional environment(s): inferences from the first evidence on microcoprolites from India. *Acta Geologica Sinica* **94**:1574-1590 DOI 10.1111/1755-6724.14293.

Kasiński JR, Badura J, Pańczyk M, Pécskay Z, Saternus A, Słodkowska B, Urbański P. 2015. Osady paleogeńskie w polskiej części niecki żytawskiej-nowe światło na problem wieku zapadliska tektonicznego. *Biuletyn Państwowego Instytutu Geologicznego* **461**:295-324 DOI 10.5604/08676143.1142104.

Knaust D, Hoffmann R. 2020. The ichnogenus *Lumbricaria* Munster from the Upper Jurassic of Germany interpreted as faecal strings of ammonites. *Papers in Palaeontology* **7**:807-823 DOI 10.1002/spp2.1311.

Kotlarczyk J, Jerzmańska A, Świdnicka E, Wiszniowska T. 2006. A framework of ichthyofaunal ecostratigraphy of the Oligocene-Early Miocene strata of the Polish Outer Carpathian basin. *Annales Societatis Geologorum Poloniae* **76**:1-111

Kovalchuk O, Nadachowski A, Świdnicka E, Stefaniak K. 2019. Fishes from the Miocene lacustrine sequence of Bełchatów (Poland). *Historical Biology* **32**:1011-1018 DOI 10.1080/08912963.2018.1561671.

Kowalski K, Rzebik-Kowalska B. 2002. Paleoecology of the Miocene fossil mammal fauna from Bełchatów (Poland). *Acta Theriologica* **47, Suppl. 1**:115-126 DOI 10.1007/BF03192483.

Krzyszkowski D. 1989. The tectonic deformation of Quaternary deposits within the Kleszczów Graben, central Poland. *Tectonophysics* **163**:285-287 DOI 10.1016/0040-1951(89)90263-1.

Love JD, Boyd DW. 1991. Pseudocoprolites in the Mowry Shale (Upper Cretaceous), Northwest Wyoming. *University of Wyoming Contribution to Geology* **28**:139-144

Lucas J, Prevot LE. 1991. Phosphates and fossil preservation. In: Allison P, Briggs D, eds.*Taphonomy, Releasing the Data Locked in the Fossil Record*. Plenum Press: New York. 389-409

Lukeneder A, Surmik D, Gorzelak P, Niedźwiedzki R, Brachaniec T, Salamon MA. 2020. Bromalites from the Upper Triassic Polzberg section (Austria); insights into trophic interactions and food chains of the Polzberg palaeobiota. *Scientific Reports* **10**:20545 DOI 10.1038/s41598-020-77017-x.

Musiał T. 1987. Miocen Roztocza (Polska południowo-wschodnia). *Prace Państwowego Instytutu Geologicznego* **31**:5-149

Mustoe GE. 2001. Enigmatic origin of ferruginous coprolites: evidence from the Miocene Wilkes formation, Southwestern Washington. *GSA Bulletin* **113**:673-681 DOI 10.1130/0016-7606(2001)113<0673:EOOFCE>2.0.CO;2.

Niedźwiedzki G, Bajdek P, Owocki K, Kear BP. 2016. An Early Triassic polar predator ecosystem revealed by vertebrate coprolites from the Bulgo Sandstone (Sydney Basin) of southeastern Australia. *Palaeogeography, Palaeoclimatology, Palaeoecology* **464**:5-15 DOI 10.1016/j.palaeo.2016.04.003.

Olchowy P, Krajewski M, Felisiak I. 2019. Late Jurassic facies succession of the Kleszczów Graben area (southern border of the Łódz Depression, peri-Tethyan shelf, central Poland). *Geological Quarterly* **63**:657-681 DOI 10.7306/gq.1496.

Peñalver E, Gaudant J. 2010. Limnic food weband salinity of the Upper Miocene Bicorb palaeolake (easternSpain). *Palaeogeography, Palaeoclimatology, Palaeoecology* **297**:683-696 DOI 10.1016/j.palaeo.2010.09.017.

Pesquero DM, Salesa JM, Espílez E, Mampel L, Siliceo G, Alcalá L. 2011. An exceptionally rich hyaena coprolites concentration in the Late Miocene mammal fossil site of La Roma 2 (Terual, Spain): taphonomical and palaeoenvironmental inferences. *Palaeogeography, Palaeoclimatology, Palaeoecology* **311**:30-37 DOI 10.1016/j.palaeo.2011.07.013.

Peterson CD, Madin IP. 1997. Coseismic paleoliquefaction in the central Cascadia margin USA. *Oregon Geology* **59**:51-74

Popov SV, Akhmetiev MA, Burgova EM, Lopatin AV, Amitrov OV, Andreyeva-Grigorovich AS, Zaporozhec NI, Zherikhin VV, Krasheninnikov VA, Nikolaeva IA, SytchevskayaEK, Scherba IB. 2002. Biogeography of the Northern Peri-Tethys from the Late Eocene to the Early Miocene, part 2: Early Oligocene. *Paleontological Journal* **36 (Suppl. 3)**:S185-S259

Qvarnström M, Wernström JV, Wawrzyniak Z, Barbacka M, Pacyna G, Górecki A, Ziaja J, Jarzynka A, Owocki K, Sulej T, Marynowski L, Pieńkowski G, Ahlberg PE, Niedźwiedzki G. 2024. Digestive contents and food webs record the advent of dinosaur supremacy. *Nature* **636**:397-403 DOI 10.1038/s41586-024-08265-4.

Qvarnström M, Anagnostakis S, LindskogA, Scheer U, Vajda V, Rasmussen BW, Lindgren J, Eriksson ME. 2019. Multi-proxy analyses of Late Cretaceous coprolites from Germany. *Lethaia* **52**:550-569 DOI 10.1111/let.12330.

Richter G, Baszio S. 2001. Traces of a limnic food web in the Eocene Lake Messel – a preliminary report based on fish coprolite analyses. *Palaeogeography, Palaeoclimatology, Palaeoecology* **166**:345-368 DOI 10.1016/S0031-0182(00)00218-2.

Richter G, Wedmann S. 2005. Ecology of the Eocene Lake Messel revealed by analysis of small fish coprolites and sediments from a drilling core. *Palaeogeography, Palaeoclimatology, Palaeoecology* **223**:147-161 DOI 10.1016/j.palaeo.2005.04.002.

Roberts AE. 1958. *Geology and coal resources of the Toledo-Castle Rock District, Cowlitz and Lewis Counties*. Washington, D.C.: U.S. Geological Survey Bulletin.

Román Z, Segesdi M, Sebe K, Földes T, Bakrač K, Virág A, Botfalvai G.2024. Palaeontological and taphonomical investigations of the exceptionally rich concentration of Miocene vertebrate coprolites from Pécs-Danitzpuszta (Hungary, Mecsek Mts.). *Historical Biology* **37**:663-678 DOI 10.1080/08912963.2024.2324435.

Rummy P, Halaçlar K, Chen H. 2021. The first record of exceptionally-preserved spiral coprolites from the Tsagan-Tsab formation (Lower Cretaceous), Tatal, western Mongolia. *Scientific Reports* **11**:7891 DOI 10.1038/s41598-021-87090-5.

Salamon MA, Niedźwiedzki R, Gorzelak P, Lach R, Surmik D. 2012. Bromalites from the Middle Triassic of Poland and the rise of the Mesozoic Marine Revolution. *Palaeogeography, Palaeoclimatology, Palaeoecology* **321-322**:142-150 DOI 10.1016/j.palaeo.2012.01.029.

Salamon MA, Radwańska U, Paszcza K, Krajewski M, Brachaniec T, Niedźwiedzki R, Gorzelak P. 2024. The latest shallow-sea isocrinids from the Miocene of Paratethys and implications to the Mesozoic marine revolution. *Scientific Reports* **14**: 17932 DOI 10.1038/s41598-024-67687-2.

Schweigert G, Dietl G. 2012. Vertebrate coprolites from the Nusplingen Lithographic Limestone (Upper Jurassic, SW Germany). *New Mexico Museum of Natural History & Science Bulletin* **57**:215-220

Schwimmer DR, Weems RE, Sanders AE. 2015. A Late Cretaceous shark coprolite with baby freshwater turtle vertebrae inclusions. *Palaios* **30**:707-713 DOI 10.2110/palo.2015.019.

Segesdi M., Botfalvai G, Bodor ER, Ősi A, Buczkó K, Dallos Z, Tokai R, Földes T. 2017. First report on vertebrate coprolites from the Upper Cretaceous (Santonian) Csehbánya Formation of Iharkút, Hungary.*Cretaceous Research* **74**:87-99 DOI 10.1016/j.cretres.2017.02.010.

Seilacher A, Marshall C, Skinner WC, Tsuihiji T. 2001. A fresh look at sideritic coprolites. *Paleobiology* **27**:7-13 DOI 10.1666/0094-8373(2001)027<0007:aflasc>2.0.co;2.

Spencer PK. 1993. The “coprolites” that arent: the straight poop on specimens from the Miocene of Southwestern Washington State, Ichnos. *An International Journal for Plant and Animal Traces* **2**:231-236

Spencer PK. 1997. The method of multiple working hypotheses in undergraduate education with an example of its application and misapplication. *Journal of Geoscience Education* **45**:123-128

Spencer PK, Tuttle FH. 1980. Coprolites or pseudo-coprolites? New evidence concerning theorigin of Washington coprolites. *Geological Society of America* **12**:153

Stringer GL, King L. 2012. Late Eocene shark coprolites from the Yazoo Clay in northern Louisiana.*New Mexico Museum of Natural History & Science Bulletin* **57**:275-310

Studencki W. 1999. Red-algal limestones in the Middle Miocene of the Carpathian Foredeep in Poland: facies variability and palaeoclimatic implications. *Geological Quarterly* **43**:395-404

Stworzewicz E. 1999. Miocene Land Snails From Bełchatów (Central Poland). Pupilloidea (Gastropoda Pulmonata). Systematic, Biostratigraphic And Palaeoecological Studies. *Folia Malacologica* **7**:133-170 DOI 10.12657/folmal.007.015.

Świdnicka E. 2007. *Aturia* sp. (Nautiloidea) from Oligocene of the Menilite-Krosno Series of the Polish Carpathians. In: Żylińska A, ed.*Granice Paleontologii*. Materiały XX konferencji Naukowej Paleobiologów i Biostratygrafów PTG: Warszawa. 137-138

Tolar T, Galik A. 2019. A Study of Dog Coprolite from Late Neolithic Pile-Dwelling Site in Slovenia. *Archaeological Discovery* **7**:20-29 DOI 10.4236/ad.2019.71002.

Tomassini LR, Montalvo IC, Bargo MS, Vizcaíno FS, Cuitiño IJ. 2019. Sparassodonta (Metatheria) coprolites from the early-mid Miocene (Santacrucian age) of Patagonia (Argentina) with evidence of exploitation by coprophagous insects. *Palaios* **34**:639-651 DOI 10.2110/palo.2019.080.

Vajda V, Fernández MDP, Villanueva-Amadoz U, Lehsten V, Alcalá L. 2016. Dietary and environmental implications of Early Cretaceous predatory dinosaur coprolites from Teruel, Spain. *Palaeogeography, Palaeoclimatology, Palaeoecology* **464**:134-142 DOI 10.1016/j.palaeo.2016.02.036.

Wang X, White SC, Balisi M, Biewer J, Sankey J, Garber D, Tseng ZJ. 2018. First bone-cracking dog coprolites provide new insight into bone consumption in Borophagus and their unique ecological niche. *eLife* **7**:e34773 DOI 10.7554/eLife.34773.

Wetmore A. 1943. The occurrence of feather impressions in the Miocene deposits of Maryland. *The Auk* **60**:440-441

Widera M, Klęsk J, Urbański P. 2024. The geology of the deepest Cenozoic lignite-rich grabens in Poland with particular reference to their lithostratigraphy: a comparative study. *Geology, Geophysics & Environment* **50**:131-143 DOI 10.7494/geol.2024.50.2.131.

Wilson MVH. 1987. Predation as a source of fish fossils in Eocene lake sediment. *Palaios* **2**:497-504 DOI 10.2307/3514620.

Wood JR, Wilmshrust J. 2014. Late Quaternary terrestrial vertebrate coprolites from New Zealand. *Quaternary Science Reviews* **98**:33-34 DOI 10.1016/j.quascirev.2014.05.020.

Wood JR, Wilmshrust J. 2016. A protocol for subsampling Late Quaternary coprolites for multi-proxy analysis. *Quaternary Science Reviews* **138**:1-5 DOI 10.1016/j.quascirev.2016.02.018.

Wysocka A, Jasionowski M, Peryt TM. 2007. Miocen Roztocza. Miocene of the Roztocze Hills. *Biuletyn Państwowego Instytutu Geologicznego* **422**:79-96

Zatoń M, Niedźwiedzki G, Marynowski L, Benzerara K, Pott C, Cosmidis J, Krzykawski T, Filipiak P. 2015. Coprolites of Late Triassic carnivorous vertebrates from Poland: an integrative approach. *Palaeogeography, Palaeoclimatology, Palaeoecology* **430**:21-46 DOI 10.1016/j.palaeo.2015.04.009.

Figures captions

Figure 1. Geological settings of studied locations. (A). Map of Poland with marked research areas. **(B).** Kleszczów Graben area. **(C).** Southern edge of the Holy Cross Mountains. **(D).** Turów area. **(E).** Roztocze. **(F).** Menilite-Krosno Series of the Outer Carpathians. **(G).** Stratigraphic section andpositions of sites where the coprolites have been documented. Compiled and slightly modified after: *Kotlarczyk et al., 2006; Wysocka, Jasionowski & Peryt, 2007; Olchowy, Krajewski & Felisiak, 2019; Brachaniec et al., 2022; Salamon et al., 2024*.

Figure 2. Examples of coprolites collected in the Oligocene and Miocene marine sediments of Poland. Kąkolówka I:(**A**) GIUS 10–3796/O/2; (**B**) GIUS 10–3796/O/7; (**C**) GIUS 10–

3796/O/23; Kąkolówka II: (**D**) GIUS 10–3796/O/154; (**E**) GIUS 10–3796/O/181; (**F**) Kąkolowka I, GIUS 10–3796/O/60; (**G**) Kąkolówka I, GIUS 10–3796/O/77; Wola Czudecka: (**H**) GIUS 10–3796/O/251; (**I**) GIUS 10–3796/O/253; (**J**) GIUS 10–3796/O/259; (**K**) GIUS 10–3796/O/274; (**L**) Futoma, GIUS 10–3796/O/279; (**M**) Futoma, GIUS 10–3796/O/282; Kąkolówka I: (**N**) GIUS 10–3796/O/96; (**O**) GIUS 10–3796/O/98; (**P**) GIUS 10–3796/O/107; (**R**) GIUS 10–3796/O/111;(**S**) GIUS 10–3796/O/135; (**T**) Jamna Dolna, GIUS 10–3796/O/294; (**U**) Kąkolówka I, GIUS 10–3796/O/139. Scale bars 5 mm.

Figure 3. Examples of coprolites collected in Oligocene and Miocene marine. (**A-D**) and non-marine (**E-N**) sediments of Poland. Równe: (**A**) GIUS 10–3796/O/297; Jasienica Rosielna (**B**) GIUS 10–3796/O/299; Kąkolówka I (**C**) GIUS 10–3796/O/144; Temeszów (**D**) GIUS 10–3796/M/33; Gochułów (**E**) GIUS 10–3796/M/13; Roztocze area-Żelebsko (**F**) GIUS 10–3796/M/32; Turów area (**G**) GIUS 10–3796/M/16; (**H**) GIUS 10–3796/M/19; (**I**) GIUS 10–3796/M/23; (**J**) GIUS 10–3796/M/28; (**K**) GIUS 10–3796/M/30; Bełchatów (**L**) GIUS 10–3796/M/2; (**M**) GIUS 10–3796/M/6; (**N**) GIUS 10–3796/M/11. Scale bars 5 mm.

Figure 4. BSE images of investigated coprolites from Oligocene coprolites of the Menilite-Krosno Series of the Outer Carpathians. (**A-E, J**) Fish bones. (**F-I?**) Scales. (**K-L**) Teeth. (**A-B, D, E, G-I**) Kąkolówka I locality, GIUS 10–3796/O/107; (**C**) Jasienica Rosielna locality, GIUS 10–3796/O/300; (**F, J-L**) Jamna Dolna locality, GIUS10–3796/O/294. Scale bars 30 um.

Figure 5. BSE images showing unidentified fossil bone remains embedded within coprolite matrix from Miocene of the Menilite-Krosno Series of the Outer Carpathians (GIUS 10–3796/M/33 and 34 respectively). (**A**) The coprolite/matrix boundary and the surrounding sediment, with bone fragments visible in both. (**B**) Remains of different morphology. (**C-E**) Close-ups of selected fossilized fragments. Scale bars 200 um.

Figure 6. Recent faeces. (**A**) Brown hare (*Lepus europeaus*). (**B**) European mole (*Talpa europaea*). (**C**) Guinea pig (*Cavia porcellus*). (**D**) Swinhoe's striped squirrel (*Tamiops swinhoei*). (**E**) Seba's short-tailed bat (*Carollia perspicillata*). (**F**) House sparrow (*Passer domesticus*). (**G**) Syngnathidae. (**H**) City pigeon (*Columba livia forma urbana*). (**I**) Zebra moray (*Gymnomuraena zebra*). (**J**) Hermit crab (*Coenobita brevimanus*). (**K**) Flying crab (*Liocarcincus holsatus*). (**L**) Sea cucumber (*Holothuria* sp.; redrawn from *Knaust & Hoffmann, 2020*). (**M**) Cephalopod (*Nautilus pompilius*; redrawn from *Knaust & Hoffmann, 2020*). (**N**) Perciformes. Scale bars 1 cm.

Figure 7. Examples of crab fossils representing *Liocarcinus oligocenicus* from the Oligocene marine strata of the Menilite-Krosno Series (The Outer Carpathians, Poland). (**A**) Kr.J-7. (**B**) Kr.H-1. (**C**) Kr.JR-2. (**D**) Kr.J-3. (**E**) Kr.J-11. (**F**) Kr.J-16. (**G**) Kr.J-12. (**H**) Kr.J-6. (**I**) Kr.J-3. Scale bar equals 1 cm.

Figure 8. Examples of fossil fish from the Oligocene marine strata of ofthe Menilite-Krosno Series (The Outer Carpathians, Poland). (**A**) Specimen representing unidentified taxa, Ma 31. (**B**) *Clupea* sp., ROJ-215. (**C**) Specimen representing unidentified taxa,ROJ-212. (**D**) Specimen representing unidentified taxa, ROL-305. (**E**) Specimen representing unidentified taxa, ROJ-307. (**F**) *Eomyctophum* sp., Ma-52. (**G**) *Holosteus* sp., ROJR-170. (**H**) Unidentified taxa of Scombridaefamily, ROL-47. (**I**) *Centriscus* sp., ROJ-514. (**J**) *Argyropelecus* sp., ROL-221. (**K**) *Hipposyngnathus* sp., ROJ-211. (**L**) Specimen representing unidentified taxa, ROL-328. Scale bar equals 1 cm.

Figure 9. Examples of fossil fish from the Oligocene marine strata of the Menilite-Krosno Series (The Outer Carpathians, Poland). (A) *Holosteus* sp., ROJ-17. **(B)** *Holosteus* sp., ROJ-22. **(C)** *Holosteus* sp., ROJ-45. **(D)** *Oligoserranoides* sp., ROR-153. **(E)** *Oligoserranoides* sp., ROJ-47. **(F)** *Oligoserranoides* sp., RORR-7. Scale bar equals 1 cm.

Figure 10. Examples of fossil fish collected in Oligocene marine strata ofthe Menilite-Krosno Series (The Outer Carpathians, Poland). (**A**) *Scopeloides* sp. GIUS10–3796/O/F1. (**B**) Jaw of *Lepidopus* sp. (**C, D**) probably *Scopeloides* sp. GIUS10–3796/O/F3, 4. Scale bar equals 1 cm.

Figure 11. Examples of fossil fish from the Oligocene marine strata ofthe Menilite-Krosno Series (The Outer Carpathians, Poland). (**A**) *Lepidopus* sp., ROU-400. (**B**) *Lepidopus* sp., ROU-405. (**C**) *Lepidopus* sp., Ma-5. (**D**) *Lepidopus* sp., ROU-40. (**E**) *Lepidopus* sp., ROU-42. (**F**) *Lepidopus* sp., ROL-55. (**G**) *Isurus* sp., ROM-ZR-100.(**H**) *Isurus* sp., ROM-ZR-103. (**I**) *Isurus* sp., ROM-ZR-107. (**J**) *Isurus* sp., ROM-ZR-112. (**K**) *Isurus* sp., ROJ-ZR-123. Scale bar equals 1 cm.

Figure 12. Examples of feathers representing unidentified taxa from the Oligocene marine strata of the Menilite-Krosno Series (The Outer Carpathians, Poland). (**A**) MSMD.Av. Jam-11. (**B**) MSMD.Av. Jam-14. (**C**) MSMD.Av. S.Bir-3. (**D**) MSMD.Av. Jam-1. (**E**) MSMD.Av. J.Ros-9. (**F**) MSMD.Av. Jam-15. Scale bar equals 1 cm.

Figure 13. Some examples of vertebrate remains documented in Miocenian deposits of the Kleszczów Graben, central Poland. Acronyme number: GIUS 10–3796V. (**A**) Jaw of a Lacertidae lizard. (**B**) Otolith of *Klingobius andjelkocae*. (**C, D**) Vertebrae of indeterminated rodents. (**E–H**) Bones of indeterminate vertebrates. (**I**) Jaw of a rodent. (**J**) Tooth of Chiroptera. (**K**) Incisor of Castocrinae. (**L–N**) Talpidaeteeth. (**O**) Tooth of an unidentified predator. Scale bar equals 1 mm.

Figure 1

Geological settings of studied locations.

(A). Map of Poland with marked research areas. (B). Kleszczów Graben area. (C). Southern edge of the Holy Cross Mountains. (D). Turów area. (E). Roztocze. (F). Menilite-Krosno Series of the Outer Carpathians. (G). Stratigraphic section andpositions of sites where the coprolites have been documented. Compiled and slightly modified after: *Kotlarczyk et al., 2006; Wysocka, Jasionowski & Peryt, 2007; Olchowy, Krajewski & Felisiak, 2019; Brachaniec et al., 2022; Salamon et al., 2024*.

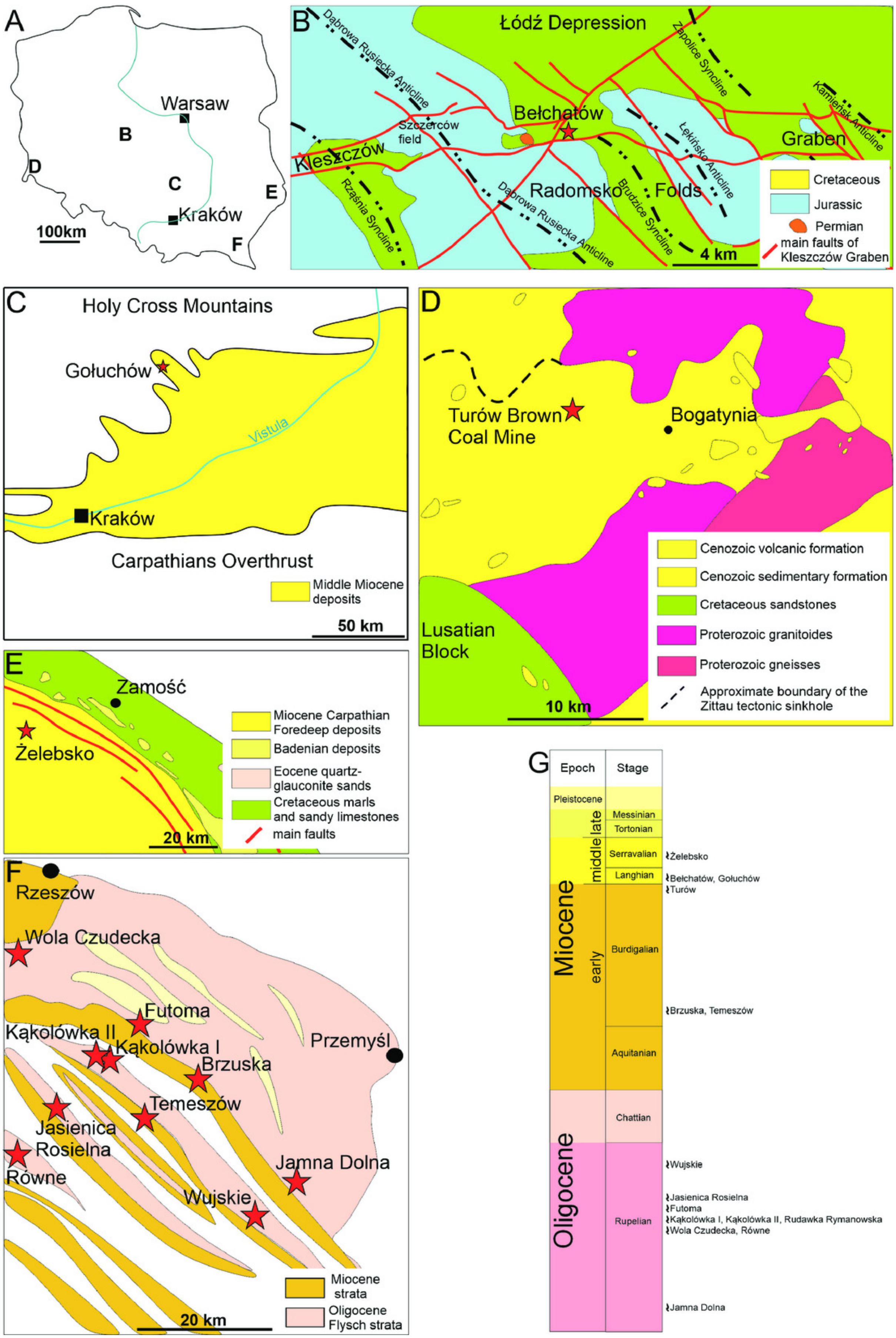
A
Warsaw
B
C
D
E
Kraków
F
100km
B
Łódź Depression
Dąbrowa Rusiecka Anticline
Zapolice Syncline
Kamieńsk Anticline
Szczerców field
Bełchatów
Graben
Kleszczów
Łękińsko Anticline
Rząśnia Syncline
Radomsko
Folds
Dąbrowa Rusiecka Anticline
Brudzice Syncline
4 km
Cretaceous
Jurassic
Permian
main faults of Kleszczów Graben
C
Holy Cross Mountains
Gołuchów
Vistula
Kraków
Carpathians Overthrust
Middle Miocene deposits
50 km
D
Turów Brown Coal Mine
Bogatynia
Lusatian Block
10 km
Cenozoic volcanic formation
Cenozoic sedimentary formation
Cretaceous sandstones
Proterozoic granitoides
Proterozoic gneisses
Approximate boundary of the Zittau tectonic sinkhole
E
Zamość
Żelebsko
20 km
Miocene Carpathian Foredeep deposits
Badenian deposits
Eocene quartz-glauconite sands
Cretaceous marls and sandy limestones
main faults
F
Rzeszów
Wola Czudecka
Futoma
Kąkolówka II
Kąkolówka I
Brzuska
Przemyśl
Temeszów
Jasienica Rosielna
Równe
Jamna Dolna
Wujskie
20 km
Miocene strata
Oligocene Flysch strata
G
Epoch
Stage
Pleistocene
Miocene
late
middle
early
Messinian
Tortonian
Serravalian
Langhian
Burdigalian
Aquitanian
Oligocene
Chattian
Rupelian
Żelebsko
Bełchatów, Gołuchów
Turów
Brzuska, Temeszów
Wujskie
Jasienica Rosielna
Futoma
Kąkolówka I, Kąkolówka II, Rudawka Rymanowska
Wola Czudecka, Równe
Jamna Dolna

Figure 2

Examples of coprolites collected in the Oligocene and Miocene marine sediments of Poland.

Kąkolówka I: (A) GIUS 10–3796/O/2; (B) GIUS 10–3796/O/7; (C) GIUS 10–3796/O/23; Kąkolówka II: (D) GIUS 10–3796/O/154; (E) GIUS 10–3796/O/181; (F) Kąkolowka I, GIUS 10–3796/O/60; (G) Kąkolówka I, GIUS 10–3796/O/77; Wola Czudecka: (H) GIUS 10–3796/O/251; (I) GIUS 10–3796/O/253; (J) GIUS 10–3796/O/259; (K) GIUS 10–3796/O/274; (L) Futoma, GIUS 10–3796/O/279; (M) Futoma, GIUS 10–3796/O/282; Kąkolówka I: (N) GIUS 10–3796/O/96; (O) GIUS 10–3796/O/98; (P) GIUS 10–3796/O/107; (R) GIUS 10–3796/O/111;(S) GIUS 10–3796/O/135; (T) Jamna Dolna, GIUS 10–3796/O/294; (U) Kąkolówka I, GIUS 10–3796/O/139. Scale bars 5 mm.

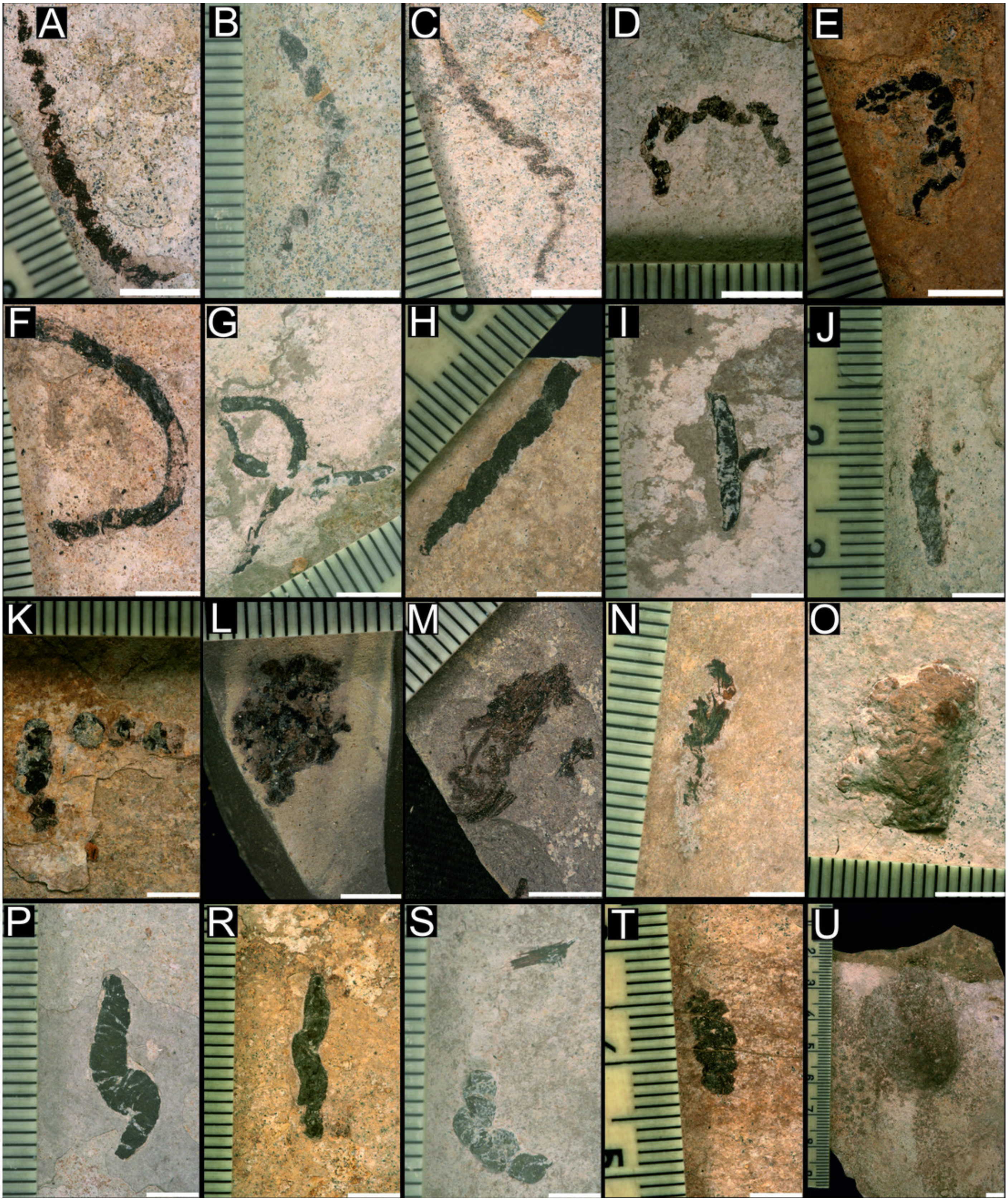
A
B
C
D
E
F
G
H
I
J
K
L
M
N
O
P
R
S
T
U

Figure 3

Examples of coprolites collected in Oligocene and Miocene marine.

(A-D) and non-marine (E-N) sediments of Poland. Równe: (A) GIUS 10–3796/O/297; Jasienica Rosielna (B) GIUS 10–3796/O/299; Kąkolówka I (C) GIUS 10–3796/O/144; Temeszów (D) GIUS 10–3796/M/33; Gochułów (E) GIUS 10–3796/M/13; Roztocze area-Żelebsko (F) GIUS 10–3796/M/32; Turów area (G) GIUS 10–3796/M/16; (H) GIUS 10–3796/M/19; (I) GIUS 10–3796/M/23; (J) GIUS 10–3796/M/28; (K) GIUS 10–3796/M/30; Bełchatów (L) GIUS 10–3796/M/2; (M) GIUS 10–3796/M/6; (N) GIUS 10–3796/M/11. Scale bars 5 mm.

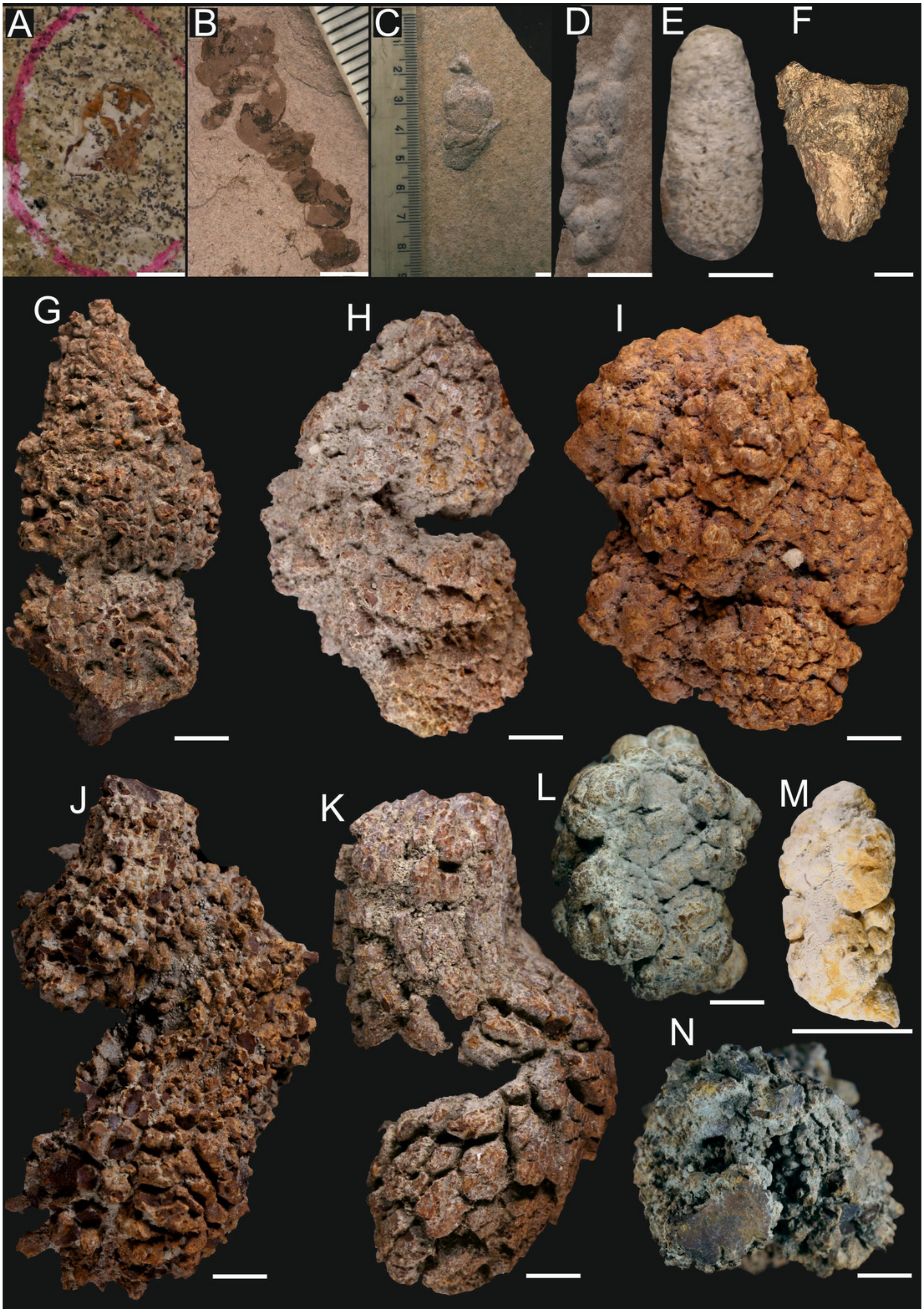
A
B
C
D
E
F
G
H
I
J
K
L
M
N

Figure 4

BSE images of investigated coprolites from Oligocene coprolites of the Menilite-Krosno Series of the Outer Carpathians.

(A - E, J) Fish bones. (F-I?) Scales. (K-L) Teeth. (A-B, D, E, G-I) Kąkolówka I locality, GIUS 10–3796/O/107; (C) Jasienica Rosielna locality, GIUS 10–3796/O/300; (F, J-L) Jamna Dolna locality, GIUS10–3796/O/294. Scale bars 30 um.

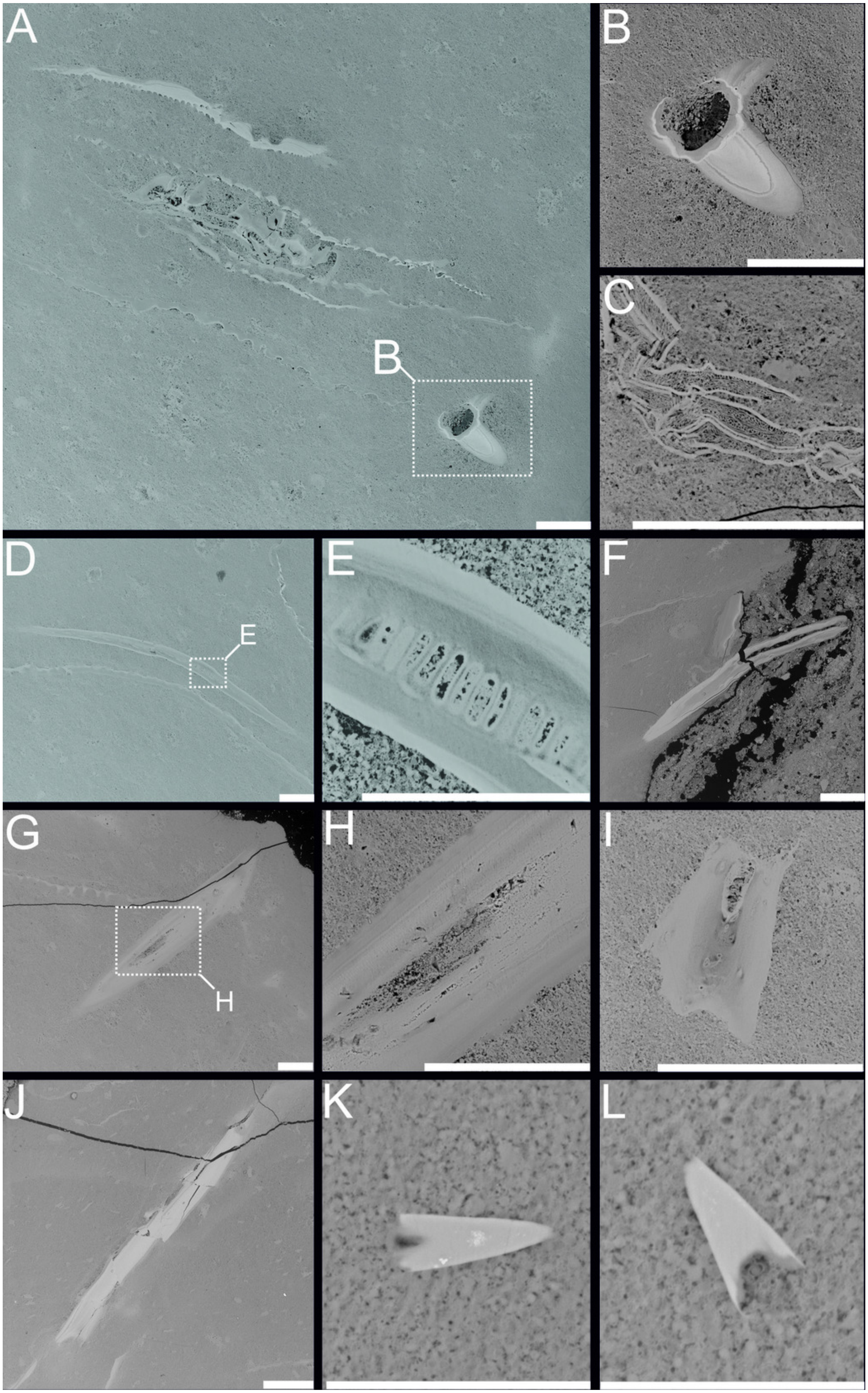
A
B
C
B
D
E
F
E
G
H
I
H
J
K
L

Figure 5

BSE images showing unidentified fossil bone remains embedded with in coprolite matrix from Miocene of the Menilite-Krosno Series of the Outer Carpathians (GIUS 10–3796/M/33 and 34 respectively).

(A) T he coprolite/matrix boundary and the surrounding sediment, with bone fragments visible in both. (B) Remains of different morphology . (C-E) Close-ups of selected fossilized fragments. Scale bars 200 um.

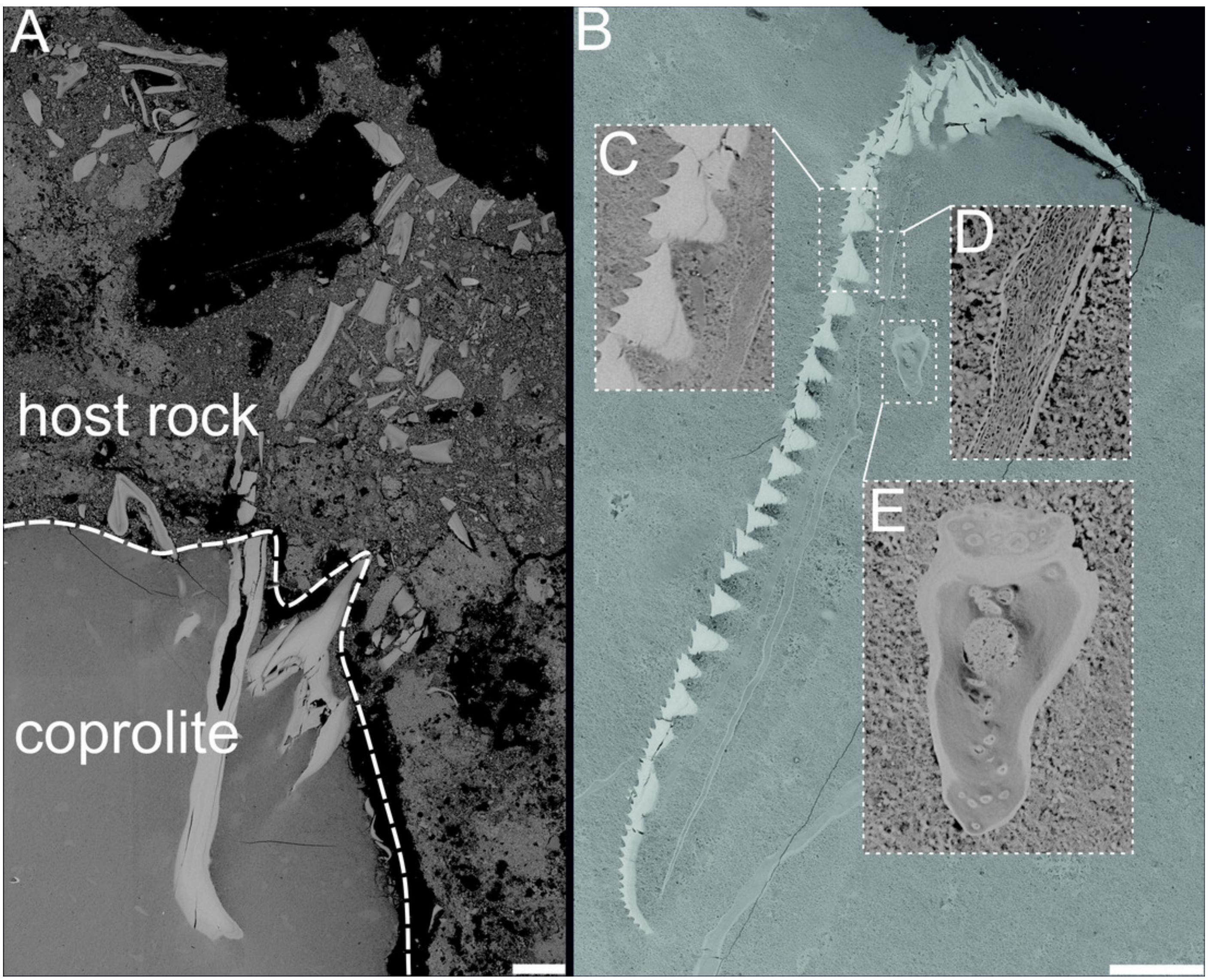

Figure 6

Recent faeces.

(A) Brown hare (*Lepus europeaus*). (B) European mole (*Talpa europaea*). (C) Guinea pig (*Cavia porcellus*). (D) Swinhoe's striped squirrel (*Tamiops swinhoei*). (E) Seba's short-tailed bat (*Carollia perspicillata*). (F) House sparrow (*Passer domesticus*). (G) Syngnathidae. (H) City pigeon (*Columba livia forma urbana*). (I) Zebra moray (*Gymnomuraena zebra*). (J) Hermit crab (*Coenobita brevimanus*). (K) Flying crab (*Liocarcincus holsatus*) . (L) Sea cucumber (*Holothuria* sp.; redrawn from *Knaust & Hoffmann, 2020*). (M) Cephalopod (*Nautilus pompilius*; redrawn from *Knaust & Hoffmann, 2020*). (N) Perciformes . Scale bars 1 cm.

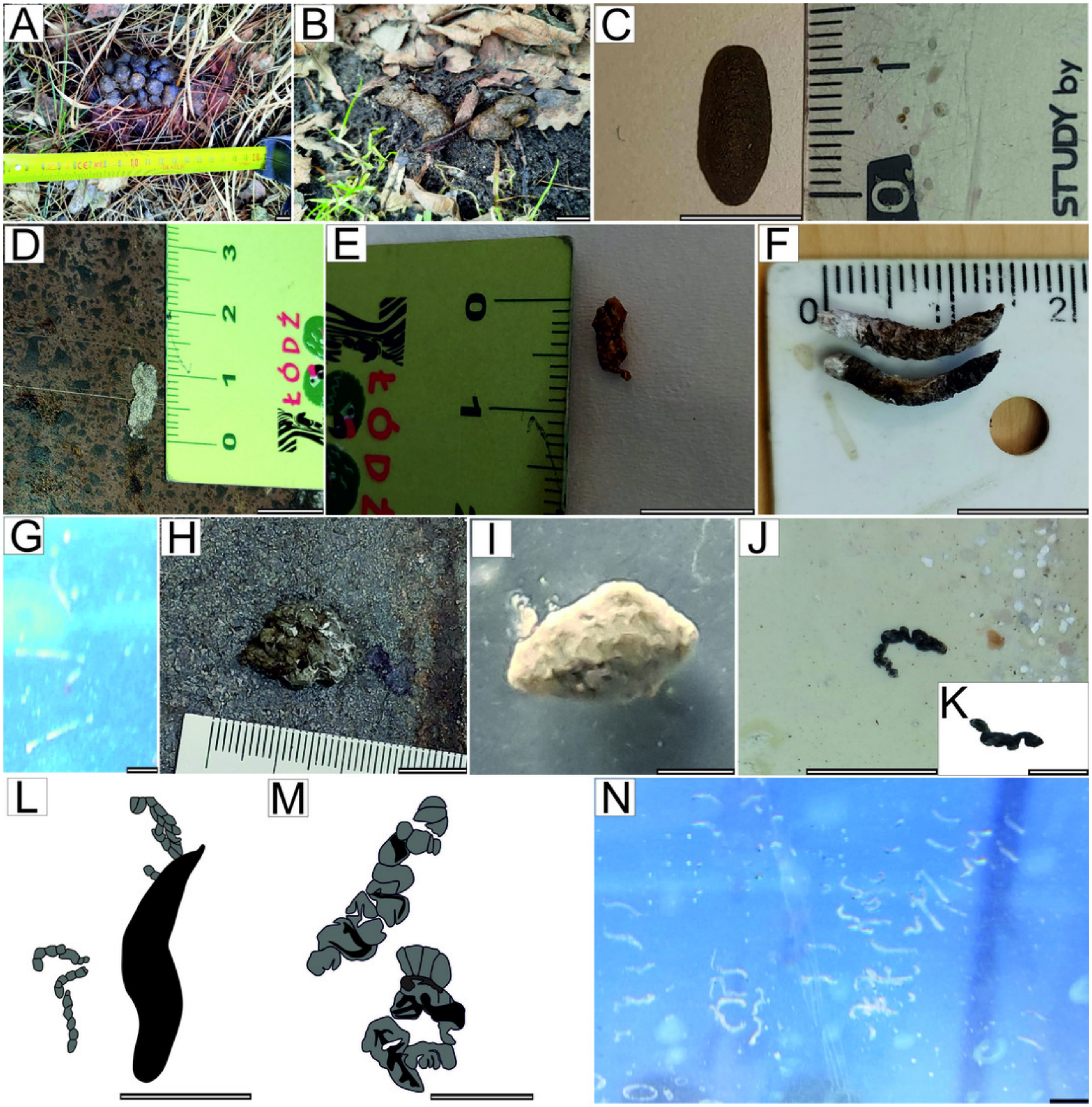
A
B
C
D
E
F
G
H
I
J
K
L
M
N
STUDY by
ŁÓDŹ

Figure 7

Examples of crab fossils representing Liocarcinus oligocenicus from the Oligocene marine strata of the Menilite-Krosno Series (The Outer Carpathians , Poland).

(A) Kr.J-7. (B) Kr.H-1. (C) Kr.JR-2. (D) Kr.J-3. (E) Kr.J-11. (F) Kr.J-16. (G) Kr.J-12. (H) Kr.J-6. (I) Kr.J-3. Scale bar equals 1 cm.

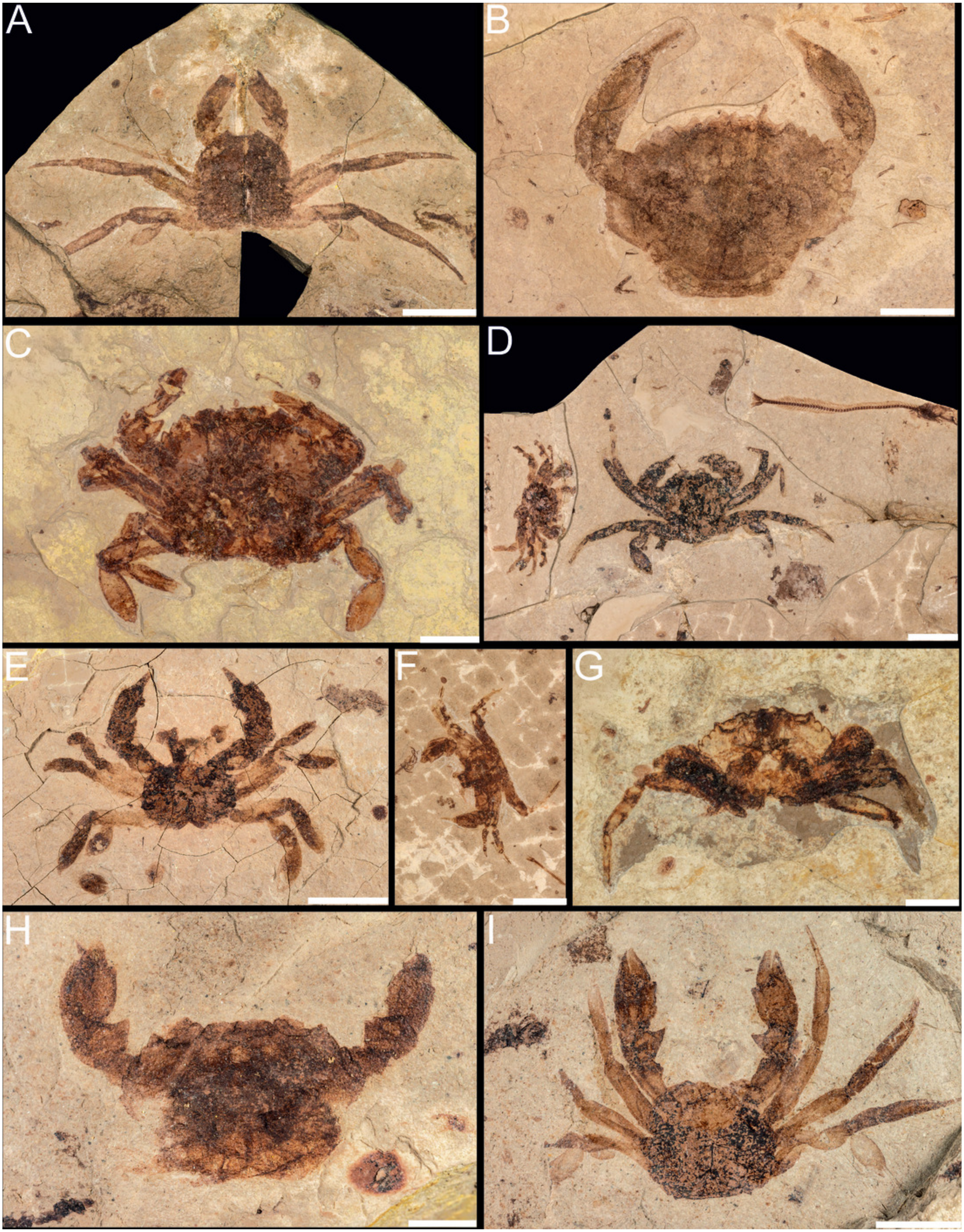
A
B
C
D
E
F
G
H
I

Figure 8

Examples of fossil fish from the Oligocene marine strata of of t he Menilite-Krosno Series (T he Outer Carpathians , Poland).

(A) Specimen representing u nidentified taxa , Ma 31. (B) *Clupea* sp., ROJ-215. (C) Specimen representing u nidentified taxa ,ROJ-212. (D) Specimen representing u nidentified taxa , ROL-305. (E) Specimen representing u nidentified taxa , ROJ-307. (F) *Eomyctophum* sp., Ma-52. (G) *Holosteus* sp., ROJR-170. (H) Unidentified taxa of Scombridae family, ROL-47. (I) *Centriscus* sp., ROJ-514. (J) *Argyropelecus* sp., ROL-221. (K) *Hipposyngnathus* sp., ROJ-211. (L) Specimen representing u nidentified taxa , ROL-328. Scale bar equals 1 cm.

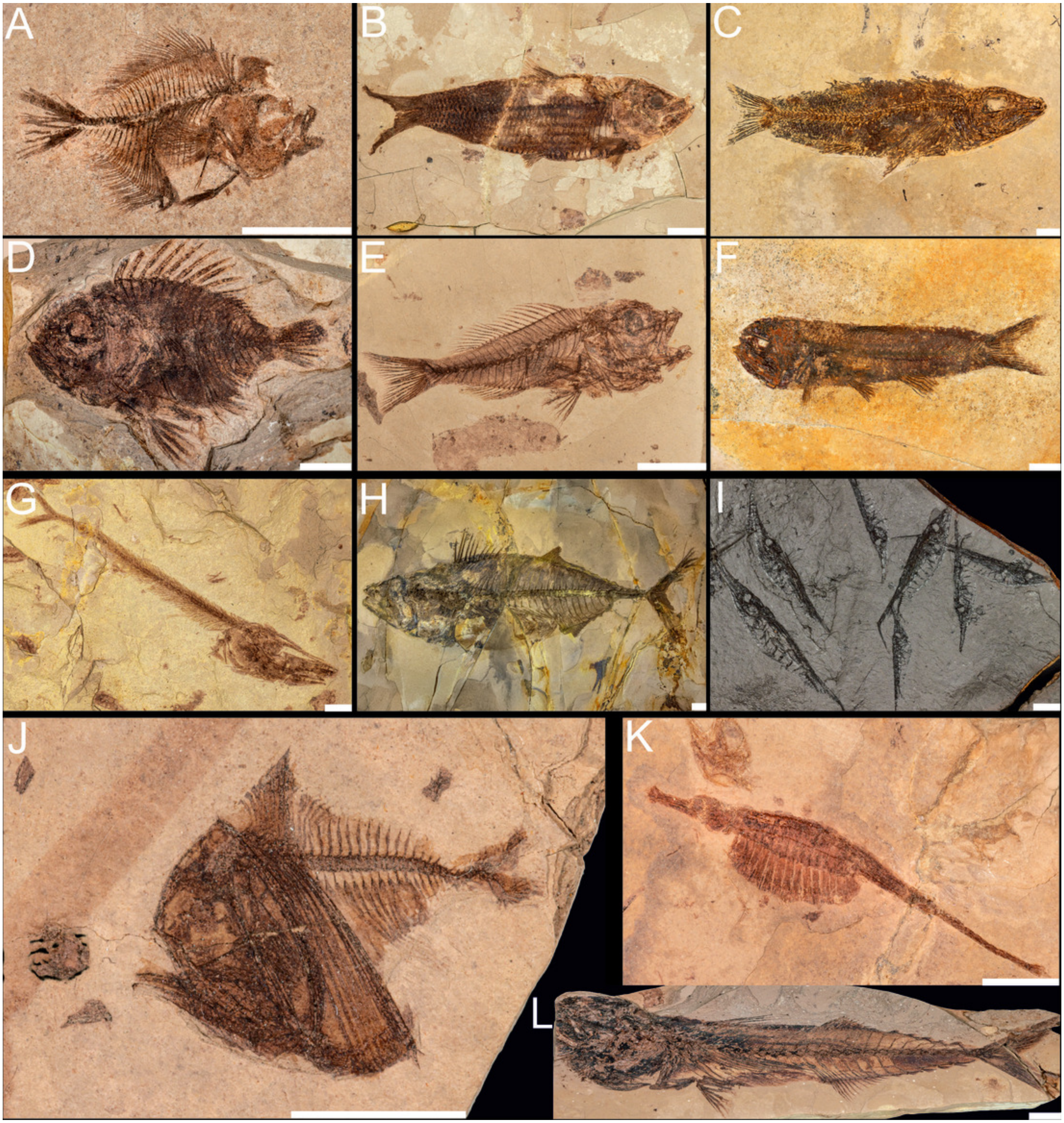
A
B
C
D
E
F
G
H
I
J
K
L

Figure 9

Examples of fossil fish from the Oligocene marine strata of the Menilite-Krosno Series (The Outer Carpathians , Poland).

(A) *Holosteus* sp., ROJ-17. (B) *Holosteus* sp., ROJ-22. (C) *Holosteus* sp., ROJ-45. (D) *Oligoserranoides* sp., ROR-153. (E) *Oligoserranoides* sp., ROJ-47. (F) *Oligoserranoides* sp., RORR-7. Scale bar equals 1 cm.

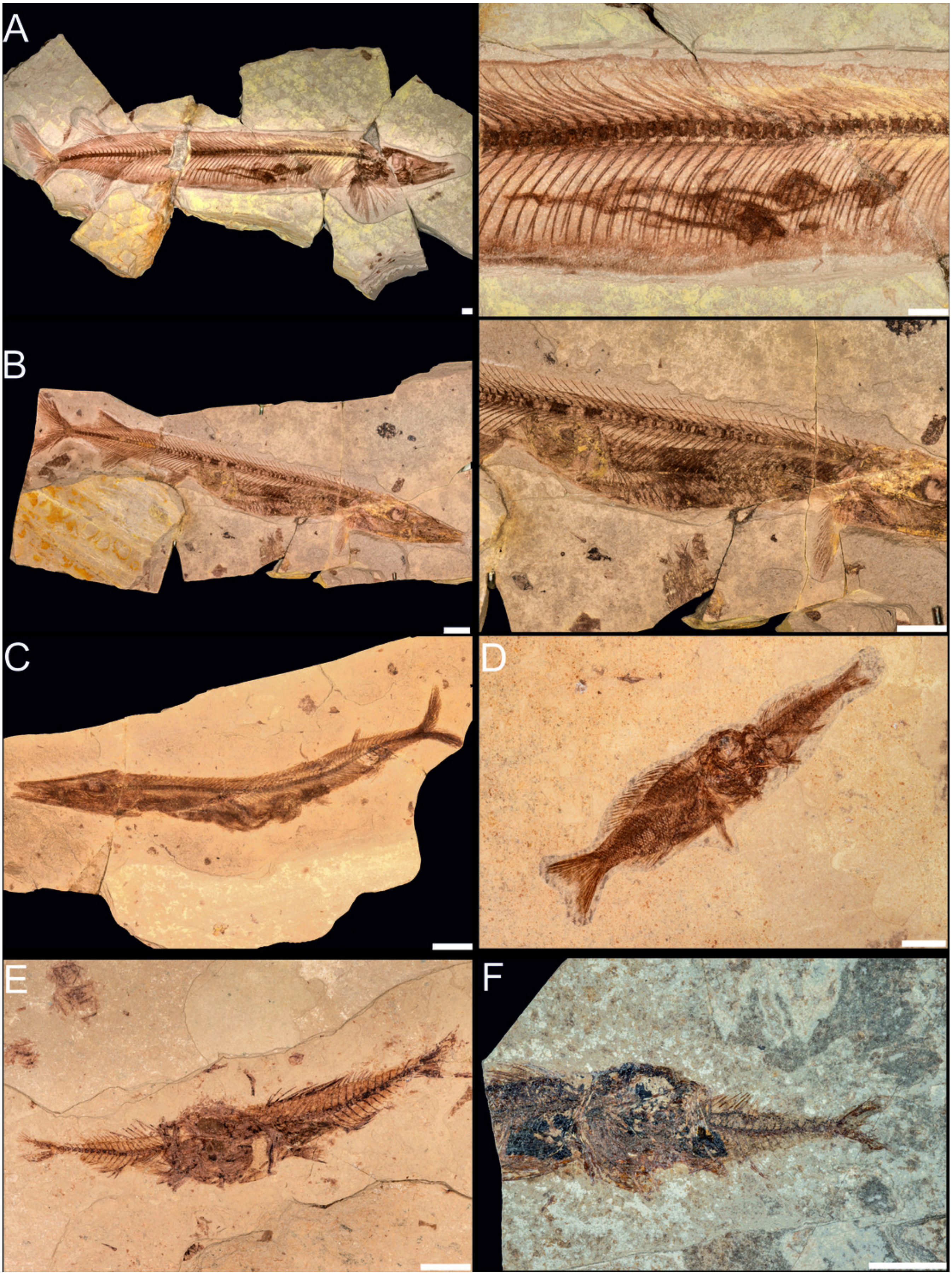
A
B
C
D
E
F

Figure 10

Examples of fossil fish collected in Oligocene marine strata of the Menilite-Krosno Series (T he Outer Carpathians , Poland).

(A) *Scopeloides* sp. GIUS10–3796/O/F1. (B) Jaw of *Lepidopus* sp. (C, D) probably *Scopeloides* sp. GIUS10–3796/O/F3, 4. Scale bar equals 1 cm.

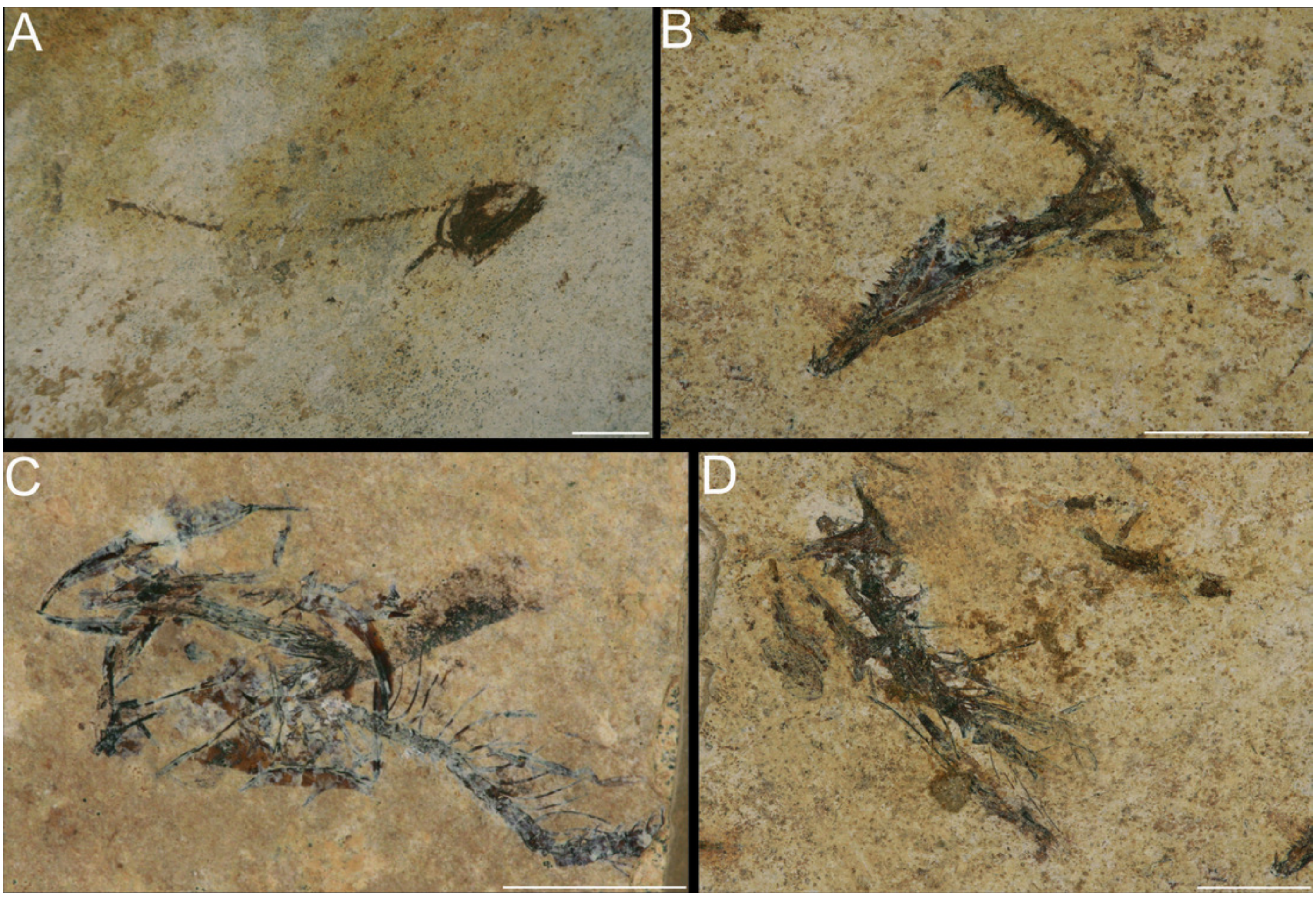

Figure 11

Examples of fossil fish from the Oligocene marine strata of the Menilite-Krosno Series (The Outer Carpathians , Poland).

(A) *Lepidopus* sp., ROU-400. (B) *Lepidopus* sp., ROU-405. (C) *Lepidopus* sp., Ma-5. (D) *Lepidopus* sp., ROU-40. (E) *Lepidopus* sp., ROU-42. (F) *Lepidopus* sp., ROL-55. (G) *Isurus* sp., ROM-ZR-100.(H) *Isurus* sp., ROM-ZR-103. (I) *Isurus* sp., ROM-ZR-107. (J) *Isurus* sp., ROM-ZR-112. (K) *Isurus* sp., ROJ-ZR-123. Scale bar equals 1 cm.

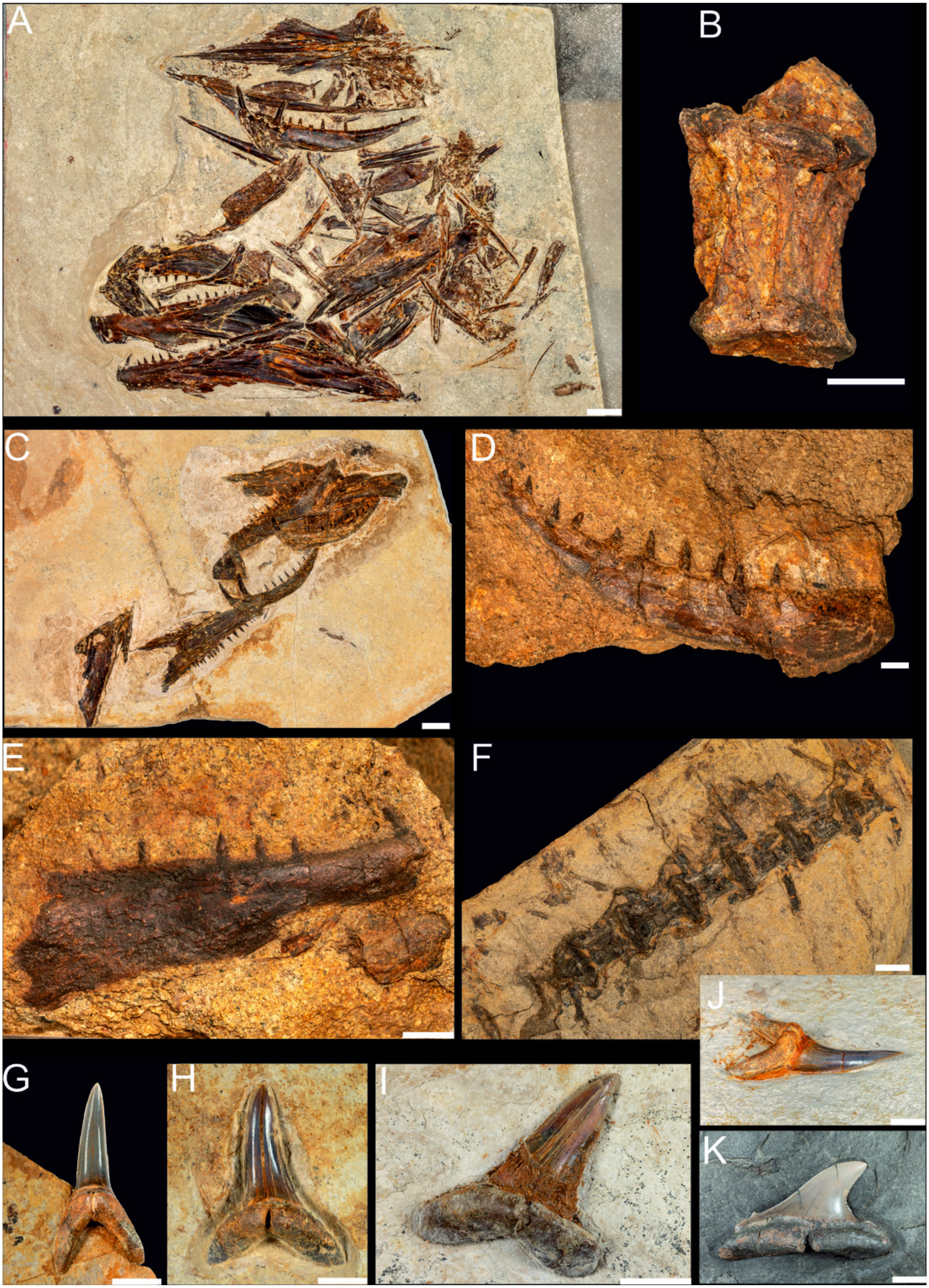
A
B
C
D
E
F
G
H
I
J
K

Figure 12

Examples of feathers representing unidentified taxa from the Oligocene marine strata of the Menilite-Krosno Series (T he Outer Carpathians , Poland) .

(A) MSMD.Av. Jam-11. (B) MSMD.Av. Jam-14. (C) MSMD.Av. S.Bir-3. (D) MSMD.Av. Jam-1. (E) MSMD.Av. J.Ros-9. (F) MSMD.Av. Jam-15. Scale bar equals 1 cm.

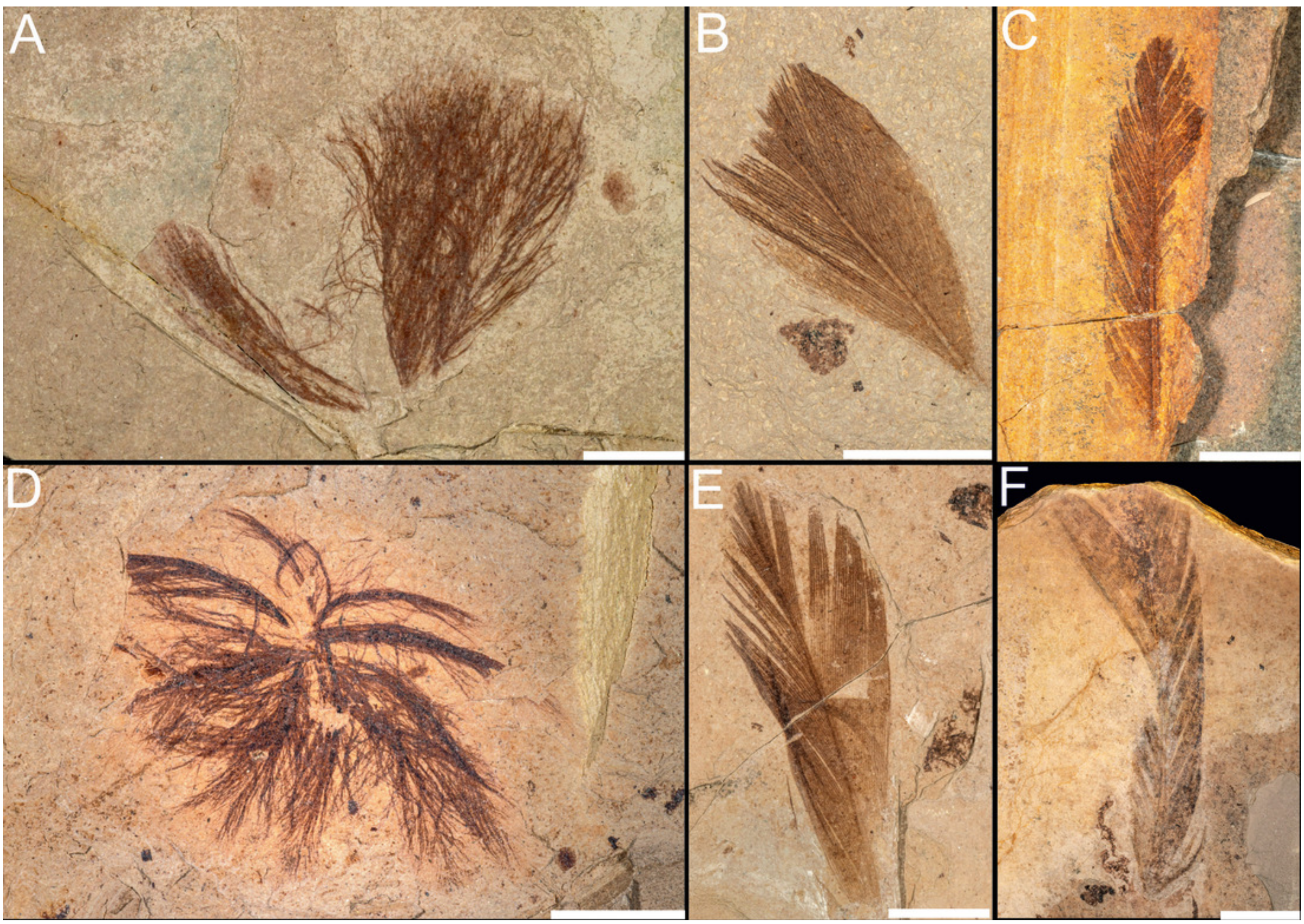

Figure 13

Some examples of vertebrate remains documented in Miocenian deposits of the Kleszczów Graben, central Poland. Acronyme number: GIUS 10–3796V.

(A) Jaw of a Lacertidae lizard. (B) Otolith of *Klingobius andjelkocae*. (C, D) Vertebrae of indeterminated rodents. (E–H) Bones of indeterminate vertebrates. (I) Jaw of a rodent. (J) Tooth of Chiroptera. (K) Incisor of Castocrinae. (L–N) Talpidaeteeth. (O) Tooth of an unidentified predator. Scale bar equals 1 mm.


A
B
C
D
E
F
G
H
I
J
K
L
M
N
O

Table 1(on next page)

Oligocene coprolite list.

Table 1:

Oligocene coprolite list.

Specimen	Dimensions (mm)	Shape	Age	Site
GIUS 10–3796/O/1	31x5	Sinusoidal	Oligocene - Rupelian	Menilite-Krosno Series (M-KS)-Kąkolówka I
GIUS 10–3796/O/2	23x3	Curved, Fig. 2a	Oligocene - Rupelian	M-KS-Kąkolówka I
GIUS 10–3796/O/3	22x5	Elongated	Oligocene - Rupelian	M-KS-Kąkolówka I
GIUS 10–3796/O/4	14x14	Oval	Oligocene - Rupelian	M-KS-Kąkolówka I
GIUS 10–3796/O/5	17x4	Sinusoidal	Oligocene - Rupelian	M-KS-Kąkolówka I
GIUS 10–3796/O/6	18x7	Curved	Oligocene - Rupelian	M-KS-Kąkolówka I
GIUS 10–3796/O/7	18x3	Curved, Fig.2b	Oligocene - Rupelian	M-KS-Kąkolówka I
GIUS 10–3796/O/8	25x10	Elongated	Oligocene - Rupelian	M-KS-Kąkolówka I
GIUS 10–3796/O/9	23x8	Elongated	Oligocene - Rupelian	M-KS-Kąkolówka I
GIUS 10–3796/O/10	38x9	Sinusoidal	Oligocene - Rupelian	M-KS-Kąkolówka I
GIUS 10–3796/O/11	24x19	Oval	Oligocene - Rupelian	M-KS-Kąkolówka I
GIUS 10–3796/O/12	17x9	Curved	Oligocene - Rupelian	M-KS-Kąkolówka I
GIUS 10–3796/O/13	23x6	S-shaped	Oligocene - Rupelian	M-KS-Kąkolówka I
GIUS 10–3796/O/14	29x8	Sinusoidal	Oligocene - Rupelian	M-KS-Kąkolówka I
GIUS 10–3796/O/15	35x11	Curved	Oligocene - Rupelian	M-KS-Kąkolówka I
GIUS 10–3796/O/16	38x10	Sinusoidal	Oligocene - Rupelian	M-KS-Kąkolówka I
GIUS 10–3796/O/17	41x9	Elongated	Oligocene - Rupelian	M-KS-Kąkolówka I
GIUS 10–3796/O/18	12x2	Sinusoidal	Oligocene - Rupelian	M-KS-Kąkolówka I
GIUS 10–	25x6	Curved	Oligocene -	M-KS-

3796/O/19			Rupelian	Kąkolówka I
GIUS 10–3796/O/20	28x14	Irregular	Oligocene - Rupelian	M-KS-Kąkolówka I
GIUS 10–3796/O/21	15x12	Oval	Oligocene - Rupelian	M-KS-Kąkolówka I
GIUS 10–3796/O/22	17x5	Elongated	Oligocene - Rupelian	M-KS-Kąkolówka I
GIUS 10–3796/O/23	32x2	Sinusoidal, Fig.2c	Oligocene - Rupelian	M-KS-Kąkolówka I
GIUS 10–3796/O/24	27x5	S-shaped	Oligocene - Rupelian	M-KS-Kąkolówka I
GIUS 10–3796/O/25	25x7	Sinusoidal	Oligocene - Rupelian	M-KS-Kąkolówka I
GIUS 10–3796/O/26	14x4	Curved	Oligocene - Rupelian	M-KS-Kąkolówka I
GIUS 10–3796/O/27	17x5	Elongated	Oligocene - Rupelian	M-KS-Kąkolówka I
GIUS 10–3796/O/28	18x17	Oval	Oligocene - Rupelian	M-KS-Kąkolówka I
GIUS 10–3796/O/29	19x6	Sinusoidal	Oligocene - Rupelian	M-KS-Kąkolówka I
GIUS 10–3796/O/30	25x15	Irregular	Oligocene - Rupelian	M-KS-Kąkolówka I
GIUS 10–3796/O/31	24x11	Sinusoidal	Oligocene - Rupelian	M-KS-Kąkolówka I
GIUS 10–3796/O/32	39x9	Elongated	Oligocene - Rupelian	M-KS-Kąkolówka I
GIUS 10–3796/O/33	26x19	Sinusoidal	Oligocene - Rupelian	M-KS-Kąkolówka I
GIUS 10–3796/O/34	15x6	Curved	Oligocene - Rupelian	M-KS-Kąkolówka I
GIUS 10–3796/O/35	22x7	S-shaped	Oligocene - Rupelian	M-KS-Kąkolówka I
GIUS 10–3796/O/36	30x28	More or less regular	Oligocene - Rupelian	M-KS-Kąkolówka I
GIUS 10–3796/O/37	14x10	More or less regular	Oligocene - Rupelian	M-KS-Kąkolówka I
GIUS 10–3796/O/38	28x11	Sinusoidal	Oligocene - Rupelian	M-KS-Kąkolówka I
GIUS 10–3796/O/39	34x10	Curved	Oligocene - Rupelian	M-KS-Kąkolówka I
GIUS 10–3796/O/40	22x9	Elongated	Oligocene - Rupelian	M-KS-Kąkolówka I
GIUS 10–3796/O/41	27x6	Sinusoidal	Oligocene - Rupelian	M-KS-Kąkolówka I
GIUS 10–	32x14	S-shaped	Oligocene -	M-KS-

3796/O/42			Rupelian	Kąkolówka I
GIUS 10–3796/O/43	25x12	Curved	Oligocene - Rupelian	M-KS-Kąkolówka I
GIUS 10–3796/O/44	16x5	Sinusoidal	Oligocene - Rupelian	M-KS-Kąkolówka I
GIUS 10–3796/O/45	34x21	Irregular	Oligocene - Rupelian	M-KS-Kąkolówka I
GIUS 10–3796/O/46	37x12	Elongated	Oligocene - Rupelian	M-KS-Kąkolówka I
GIUS 10–3796/O/47	39x9	Sinusoidal	Oligocene - Rupelian	M-KS-Kąkolówka I
GIUS 10–3796/O/48	14x13	Oval	Oligocene - Rupelian	M-KS-Kąkolówka I
GIUS 10–3796/O/49	17x7	elongated	Oligocene - Rupelian	M-KS-Kąkolówka I
GIUS 10–3796/O/50	33x9	S-shaped	Oligocene - Rupelian	M-KS-Kąkolówka I
GIUS 10–3796/O/51	32x12	Sinusoidal	Oligocene - Rupelian	M-KS-Kąkolówka I
GIUS 10–3796/O/52	30x14	Curved	Oligocene - Rupelian	M-KS-Kąkolówka I
GIUS 10–3796/O/53	26x8	Elongated	Oligocene - Rupelian	M-KS-Kąkolówka I
GIUS 10–3796/O/54	27x7	Sinusoidal	Oligocene - Rupelian	M-KS-Kąkolówka I
GIUS 10–3796/O/55	24x21	More or less regular	Oligocene - Rupelian	M-KS-Kąkolówka I
GIUS 10–3796/O/56	39x12	Sinusoidal	Oligocene - Rupelian	M-KS-Kąkolówka I
GIUS 10–3796/O/57	26x8	Curved	Oligocene - Rupelian	M-KS-Kąkolówka I
GIUS 10–3796/O/58	29x17	Irregular	Oligocene - Rupelian	M-KS-Kąkolówka I
GIUS 10–3796/O/59	37x13	S-shaped	Oligocene - Rupelian	M-KS-Kąkolówka I
GIUS 10–3796/O/60	38x4	Curved, Fig. 2f	Oligocene - Rupelian	M-KS-Kąkolówka I
GIUS 10–3796/O/61	32x12	Curved	Oligocene - Rupelian	M-KS-Kąkolówka I
GIUS 10–3796/O/62	17x16	Oval	Oligocene - Rupelian	M-KS-Kąkolówka I
GIUS 10–3796/O/63	28x9	Sinusoidal	Oligocene - Rupelian	M-KS-Kąkolówka I
GIUS 10–3796/O/64	39x15	Elongated	Oligocene - Rupelian	M-KS-Kąkolówka I
GIUS 10–	26x14	Sinusoidal	Oligocene -	M-KS-

3796/O/65			Rupelian	Kąkolówka I
GIUS 10–3796/O/66	27x13	Curved	Oligocene - Rupelian	M-KS-Kąkolówka I
GIUS 10–3796/O/67	24x10	Elongated	Oligocene - Rupelian	M-KS-Kąkolówka I
GIUS 10–3796/O/68	23x8	Curved	Oligocene - Rupelian	M-KS-Kąkolówka I
GIUS 10–3796/O/69	18x11	Irregular	Oligocene - Rupelian	M-KS-Kąkolówka I
GIUS 10–3796/O/70	19x7	Sinusoidal	Oligocene - Rupelian	M-KS-Kąkolówka I
GIUS 10–3796/O/71	28x9	S-shaped	Oligocene - Rupelian	M-KS-Kąkolówka I
GIUS 10–3796/O/72	35x14	Sinusoidal	Oligocene - Rupelian	M-KS-Kąkolówka I
GIUS 10–3796/O/73	37x12	Curved	Oligocene - Rupelian	M-KS-Kąkolówka I
GIUS 10–3796/O/74	30x29	More or less regular	Oligocene - Rupelian	M-KS-Kąkolówka I
GIUS 10–3796/O/75	50x32	Irregular	Oligocene - Rupelian	M-KS-Kąkolówka I
GIUS 10–3796/O/76	37x15	S-shaped	Oligocene - Rupelian	M-KS-Kąkolówka I
GIUS 10–3796/O/77	44x3	Curved, Fig. 2g	Oligocene - Rupelian	M-KS-Kąkolówka I
GIUS 10–3796/O/78	25x4	S-shaped	Oligocene - Rupelian	M-KS-Kąkolówka I
GIUS 10–3796/O/79	28x13	Irregular	Oligocene - Rupelian	M-KS-Kąkolówka I
GIUS 10–3796/O/80	37x8	Sinusoidal	Oligocene - Rupelian	M-KS-Kąkolówka I
GIUS 10–3796/O/81	28x20	More or less regular	Oligocene - Rupelian	M-KS-Kąkolówka I
GIUS 10–3796/O/82	24x9	S-shaped	Oligocene - Rupelian	M-KS-Kąkolówka I
GIUS 10–3796/O/83	17x5	Sinusoidal	Oligocene - Rupelian	M-KS-Kąkolówka I
GIUS 10–3796/O/84	24x6	Sinusoidal	Oligocene - Rupelian	M-KS-Kąkolówka I
GIUS 10–3796/O/85	29x11	Elongated	Oligocene - Rupelian	M-KS-Kąkolówka I
GIUS 10–3796/O/86	35x8	Sinusoidal	Oligocene - Rupelian	M-KS-Kąkolówka I
GIUS 10–3796/O/87	44x10	Irregular	Oligocene - Rupelian	M-KS-Kąkolówka I
GIUS 10–	41x15	Curved	Oligocene -	M-KS-

3796/O/88			Rupelian	Kąkolówka I
GIUS 10–3796/O/89	19x4	Sinusoidal	Oligocene - Rupelian	M-KS-Kąkolówka I
GIUS 10–3796/O/90	25x6	S-shaped	Oligocene - Rupelian	M-KS-Kąkolówka I
GIUS 10–3796/O/91	38x17	Sinusoidal	Oligocene - Rupelian	M-KS-Kąkolówka I
GIUS 10–3796/O/92	34x12	Curved	Oligocene - Rupelian	M-KS-Kąkolówka I
GIUS 10–3796/O/93	17x5	S-shaped	Oligocene - Rupelian	M-KS-Kąkolówka I
GIUS 10–3796/O/94	32x16	Irregular	Oligocene - Rupelian	M-KS-Kąkolówka I
GIUS 10–3796/O/95	37x5	Curved	Oligocene - Rupelian	M-KS-Kąkolówka I
GIUS 10–3796/O/96	21x11	Irregular	Oligocene - Rupelian	M-KS-Kąkolówka I
GIUS 10–3796/O/97	23x9	Elongated	Oligocene - Rupelian	M-KS-Kąkolówka I
GIUS 10–3796/O/98	15x6	Irregular, Fig. 2o	Oligocene - Rupelian	M-KS-Kąkolówka I
GIUS 10–3796/O/99	28x8	Curved	Oligocene - Rupelian	M-KS-Kąkolówka I
GIUS 10–3796/O/100	30x19	More or less regular	Oligocene - Rupelian	M-KS-Kąkolówka I
GIUS 10–3796/O/101	34x10	S-shaped	Oligocene - Rupelian	M-KS-Kąkolówka I
GIUS 10–3796/O/102	36x8	Sinusoidal	Oligocene - Rupelian	M-KS-Kąkolówka I
GIUS 10–3796/O/103	40x13	Curved	Oligocene - Rupelian	M-KS-Kąkolówka I
GIUS 10–3796/O/104	15x15	Oval	Oligocene - Rupelian	M-KS-Kąkolówka I
GIUS 10–3796/O/105	17x9	Sinusoidal	Oligocene - Rupelian	M-KS-Kąkolówka I
GIUS 10–3796/O/106	19x6	Elongated	Oligocene - Rupelian	M-KS-Kąkolówka I
GIUS 10–3796/O/107	24x5	S-shaped, Fig. 2p	Oligocene - Rupelian	M-KS-Kąkolówka I
GIUS 10–3796/O/108	25x4	Curved	Oligocene - Rupelian	M-KS-Kąkolówka I
GIUS 10–3796/O/109	30x14	Irregular	Oligocene - Rupelian	M-KS-Kąkolówka I
GIUS 10–3796/O/110	34x12	Elongated	Oligocene - Rupelian	M-KS-Kąkolówka I
GIUS 10–	18x4	S-shaped,	Oligocene -	M-KS-

3796/O/111		Fig. 2r	Rupelian	Kąkolówka I
GIUS 10–3796/O/112	18x7	S-shaped	Oligocene - Rupelian	M-KS-Kąkolówka I
GIUS 10–3796/O/113	15x4	Sinusoidal	Oligocene - Rupelian	M-KS-Kąkolówka I
GIUS 10–3796/O/114	37x10	S-shaped	Oligocene - Rupelian	M-KS-Kąkolówka I
GIUS 10–3796/O/115	20x16	Oval	Oligocene - Rupelian	M-KS-Kąkolówka I
GIUS 10–3796/O/116	32x9	Sinusoidal	Oligocene - Rupelian	M-KS-Kąkolówka I
GIUS 10–3796/O/117	17x11	Irregular	Oligocene - Rupelian	M-KS-Kąkolówka I
GIUS 10–3796/O/118	33x7	Elongated	Oligocene - Rupelian	M-KS-Kąkolówka I
GIUS 10–3796/O/119	29x8	Sinusoidal	Oligocene - Rupelian	M-KS-Kąkolówka I
GIUS 10–3796/O/120	22x6	Curved	Oligocene - Rupelian	M-KS-Kąkolówka I
GIUS 10–3796/O/121	41x11	Sinusoidal	Oligocene - Rupelian	M-KS-Kąkolówka I
GIUS 10–3796/O/122	31x13	Elongated	Oligocene - Rupelian	M-KS-Kąkolówka I
GIUS 10–3796/O/123	12x10	Oval	Oligocene - Rupelian	M-KS-Kąkolówka I
GIUS 10–3796/O/124	25x5	Sinusoidal	Oligocene - Rupelian	M-KS-Kąkolówka I
GIUS 10–3796/O/125	27x4	Sinusoidal	Oligocene - Rupelian	M-KS-Kąkolówka I
GIUS 10–3796/O/126	38x9	S-shape	Oligocene - Rupelian	M-KS-Kąkolówka I
GIUS 10–3796/O/127	35x7	Sinusoidal	Oligocene - Rupelian	M-KS-Kąkolówka I
GIUS 10–3796/O/128	27x25	Oval	Oligocene - Rupelian	M-KS-Kąkolówka I
GIUS 10–3796/O/129	35x10	Sinusoidal	Oligocene - Rupelian	M-KS-Kąkolówka I
GIUS 10–3796/O/130	39x8	Elongated	Oligocene - Rupelian	M-KS-Kąkolówka I
GIUS 10–3796/O/131	37x11	Curved	Oligocene - Rupelian	M-KS-Kąkolówka I
GIUS 10–3796/O/132	34x6	S-shaped	Oligocene - Rupelian	M-KS-Kąkolówka I
GIUS 10–3796/O/133	28x7	Curved	Oligocene - Rupelian	M-KS-Kąkolówka I
GIUS 10–	30x11	S-shaped	Oligocene -	M-KS-

3796/O/134			Rupelian	Kąkolówka I
GIUS 10–3796/O/135	16x5	Curved, Fig.2s	Oligocene - Rupelian	M-KS-Kąkolówka I
GIUS 10–3796/O/136	17x7	Sinusoidal	Oligocene - Rupelian	M-KS-Kąkolówka I
GIUS 10–3796/O/137	20x6	Elongated	Oligocene - Rupelian	M-KS-Kąkolówka I
GIUS 10–3796/O/138	22x13	Irregular	Oligocene - Rupelian	M-KS-Kąkolówka I
GIUS 10–3796/O/139	32x30	Oval, Fig. 2u	Oligocene - Rupelian	M-KS-Kąkolówka I
GIUS 10–3796/O/140	40x13	S-shaped	Oligocene - Rupelian	M-KS-Kąkolówka I
GIUS 10–3796/O/141	37x20	Irregular	Oligocene - Rupelian	M-KS-Kąkolówka I
GIUS 10–3796/O/142	31x15	Irregular	Oligocene - Rupelian	M-KS-Kąkolówka I
GIUS 10–3796/O/143	33x13	Curved	Oligocene - Rupelian	M-KS-Kąkolówka I
GIUS 10–3796/O/144	40x22	Irregular, Fig. 3c	Oligocene - Rupelian	M-KS-Kąkolówka I
GIUS 10–3796/O/145	43x13	S-shaped	Oligocene - Rupelian	M-KS-Kąkolówka I
GIUS 10–3796/O/146	40x10	Sinusoidal	Oligocene - Rupelian	M-KS-Kąkolówka I
GIUS 10–3796/O/147	38x9	Curved	Oligocene - Rupelian	M-KS-Kąkolówka I
GIUS 10–3796/O/148	23x10	Elongated	Oligocene - Rupelian	M-KS-Kąkolówka I
GIUS 10–3796/O/149	29x6	Elongated	Oligocene - Rupelian	M-KS-Kąkolówka I
GIUS 10–3796/O/150	17x14	Oval	Oligocene - Rupelian	M-KS-Kąkolówka I
GIUS 10–3796/O/151	14x5	Curved	Oligocene - Rupelian	M-KS-Kąkolówka II
GIUS 10–3796/O/152	30x8	S-shaped	Oligocene - Rupelian	M-KS-Kąkolówka II
GIUS 10–3796/O/153	32x5	S-shaped	Oligocene - Rupelian	M-KS-Kąkolówka II
GIUS 10–3796/O/154	14x2	Sinusoidal, Fig. 2d	Oligocene - Rupelian	M-KS-Kąkolówka II
GIUS 10–	35x8	Elongated	Oligocene -	M-KS-

3796/O/155			Rupelian	Kąkolówka II
GIUS 10–3796/O/156	22x5	Sinusoidal	Oligocene - Rupelian	M-KS-Kąkolówka II
GIUS 10–3796/O/157	32x7	S-shaped	Oligocene - Rupelian	M-KS-Kąkolówka II
GIUS 10–3796/O/158	14x3	Sinusoidal	Oligocene - Rupelian	M-KS-Kąkolówka II
GIUS 10–3796/O/159	8x6	Oval	Oligocene - Rupelian	M-KS-Kąkolówka II
GIUS 10–3796/O/160	38x6	Elongated	Oligocene - Rupelian	M-KS-Kąkolówka II
GIUS 10–3796/O/161	18x3	Sinusoidal	Oligocene - Rupelian	M-KS-Kąkolówka II
GIUS 10–3796/O/162	15x8	S-shaped	Oligocene - Rupelian	M-KS-Kąkolówka II
GIUS 10–3796/O/163	27x10	Sinusoidal	Oligocene - Rupelian	M-KS-Kąkolówka II
GIUS 10–3796/O/164	38x21	Irregular	Oligocene - Rupelian	M-KS-Kąkolówka II
GIUS 10–3796/O/165	24x9	Sinusoidal	Oligocene - Rupelian	M-KS-Kąkolówka II
GIUS 10–3796/O/166	17x8	Sinusoidal	Oligocene - Rupelian	M-KS-Kąkolówka II
GIUS 10–3796/O/167	33x6	Elongated	Oligocene - Rupelian	M-KS-Kąkolówka II
GIUS 10–3796/O/168	39x8	Curved	Oligocene - Rupelian	M-KS-Kąkolówka II
GIUS 10–3796/O/169	22x11	Irregular	Oligocene - Rupelian	M-KS-Kąkolówka II
GIUS 10–3796/O/170	41x10	Curved	Oligocene - Rupelian	M-KS-Kąkolówka

				II
GIUS 10–3796/O/171	35x13	Elongated	Oligocene - Rupelian	M-KS-Kąkolówka II
GIUS 10–3796/O/172	12x4	Sinusoidal	Oligocene - Rupelian	M-KS-Kąkolówka II
GIUS 10–3796/O/173	25x24	Oval	Oligocene - Rupelian	M-KS-Kąkolówka II
GIUS 10–3796/O/174	37x17	Elongated	Oligocene - Rupelian	M-KS-Kąkolówka II
GIUS 10–3796/O/175	15x12	Sinusoidal	Oligocene - Rupelian	M-KS-Kąkolówka II
GIUS 10–3796/O/176	19x4	Curved	Oligocene - Rupelian	M-KS-Kąkolówka II
GIUS 10–3796/O/177	19x6	S-shape	Oligocene - Rupelian	M-KS-Kąkolówka II
GIUS 10–3796/O/178	24x4	Elongated	Oligocene - Rupelian	M-KS-Kąkolówka II
GIUS 10–3796/O/179	28x7	Curved	Oligocene - Rupelian	M-KS-Kąkolówka II
GIUS 10–3796/O/180	30x8	S-shaped	Oligocene - Rupelian	M-KS-Kąkolówka II
GIUS 10–3796/O/181	11x3	Sinusoidal, Fig. 2e	Oligocene - Rupelian	M-KS-Kąkolówka II
GIUS 10–3796/O/182	33x11	Curved	Oligocene - Rupelian	M-KS-Kąkolówka II
GIUS 10–3796/O/183	19x5	Curved	Oligocene - Rupelian	M-KS-Kąkolówka II
GIUS 10–3796/O/184	20x7	Sinusoidal	Oligocene - Rupelian	M-KS-Kąkolówka II
GIUS 10–3796/O/185	15x15	Oval	Oligocene - Rupelian	M-KS-Kąkolówka II

GIUS 10–3796/O/186	37x8	Sinusoidal	Oligocene - Rupelian	M-KS-Kąkolówka II
GIUS 10–3796/O/187	46x15	Elongated	Oligocene - Rupelian	M-KS-Kąkolówka II
GIUS 10–3796/O/188	34x9	Sinusoidal	Oligocene - Rupelian	M-KS-Kąkolówka II
GIUS 10–3796/O/189	18x11	Elongated	Oligocene - Rupelian	M-KS-Kąkolówka II
GIUS 10–3796/O/190	33x6	Curved	Oligocene - Rupelian	M-KS-Kąkolówka II
GIUS 10–3796/O/191	29x6	Sinusoidal	Oligocene - Rupelian	M-KS-Kąkolówka II
GIUS 10–3796/O/192	23x7	S-shaped	Oligocene - Rupelian	M-KS-Kąkolówka II
GIUS 10–3796/O/193	42x10	Sinusoidal	Oligocene - Rupelian	M-KS-Kąkolówka II
GIUS 10–3796/O/194	37x13	Sinusoidal	Oligocene - Rupelian	M-KS-Kąkolówka II
GIUS 10–3796/O/195	17x4	Irregular	Oligocene - Rupelian	M-KS-Kąkolówka II
GIUS 10–3796/O/196	28x8	Elongated	Oligocene - Rupelian	M-KS-Kąkolówka II
GIUS 10–3796/O/197	23x4	Elongated	Oligocene - Rupelian	M-KS-Kąkolówka II
GIUS 10–3796/O/198	35x14	Curved	Oligocene - Rupelian	M-KS-Kąkolówka II
GIUS 10–3796/O/199	38x13	Curved	Oligocene - Rupelian	M-KS-Kąkolówka II
GIUS 10–3796/O/200	40x17	S-shaped	Oligocene - Rupelian	M-KS-Kąkolówka II
GIUS 10–	44x10	Elongated	Oligocene -	M-KS-

3796/O/201			Rupelian	Kąkolówka II
GIUS 10–3796/O/202	17x14	Oval	Oligocene - Rupelian	M-KS-Kąkolówka II
GIUS 10–3796/O/203	35x12	S-shaped	Oligocene - Rupelian	M-KS-Kąkolówka II
GIUS 10–3796/O/204	17x6	Sinusoidal	Oligocene - Rupelian	M-KS-Kąkolówka II
GIUS 10–3796/O/205	20x7	S-shaped	Oligocene - Rupelian	M-KS-Kąkolówka II
GIUS 10–3796/O/206	18x3	S-shaped	Oligocene - Rupelian	M-KS-Kąkolówka II
GIUS 10–3796/O/207	22x9	Elongated	Oligocene - Rupelian	M-KS-Kąkolówka II
GIUS 10–3796/O/208	26x8	Sinusoidal	Oligocene - Rupelian	M-KS-Kąkolówka II
GIUS 10–3796/O/209	38x9	Curved	Oligocene - Rupelian	M-KS-Kąkolówka II
GIUS 10–3796/O/210	24x9	Sinusoidal	Oligocene - Rupelian	M-KS-Kąkolówka II
GIUS 10–3796/O/211	17x15	Oval	Oligocene - Rupelian	M-KS-Kąkolówka II
GIUS 10–3796/O/212	23x12	Irregular	Oligocene - Rupelian	M-KS-Kąkolówka II
GIUS 10–3796/O/213	31x8	Sinusoidal	Oligocene - Rupelian	M-KS-Kąkolówka II
GIUS 10–3796/O/214	35x11	Irregular	Oligocene - Rupelian	M-KS-Kąkolówka II
GIUS 10–3796/O/215	39x13	Sinusoidal	Oligocene - Rupelian	M-KS-Kąkolówka II
GIUS 10–3796/O/216	44x9	Sinusoidal	Oligocene - Rupelian	M-KS-Kąkolówka

				II
GIUS 10–3796/O/217	12x4	Elongated	Oligocene - Rupelian	M-KS-Kąkolówka II
GIUS 10–3796/O/218	25x7	S-shaped	Oligocene - Rupelian	M-KS-Kąkolówka II
GIUS 10–3796/O/219	29x14	Sinusoidal	Oligocene - Rupelian	M-KS-Kąkolówka II
GIUS 10–3796/O/220	37x13	S-shaped	Oligocene - Rupelian	M-KS-Kąkolówka II
GIUS 10–3796/O/221	41x17	Sinusoidal	Oligocene - Rupelian	M-KS-Kąkolówka II
GIUS 10–3796/O/222	47x11	Sinusoidal	Oligocene - Rupelian	M-KS-Kąkolówka II
GIUS 10–3796/O/223	52x20	Sinusoidal	Oligocene - Rupelian	M-KS-Kąkolówka II
GIUS 10–3796/O/224	31x14	Elongated	Oligocene - Rupelian	M-KS-Kąkolówka II
GIUS 10–3796/O/225	27x26	Oval	Oligocene - Rupelian	M-KS-Kąkolówka II
GIUS 10–3796/O/226	36x13	elongated	Oligocene - Rupelian	M-KS-Kąkolówka II
GIUS 10–3796/O/227	38x15	S-shaped	Oligocene - Rupelian	M-KS-Kąkolówka II
GIUS 10–3796/O/228	16x5	S-shaped	Oligocene - Rupelian	M-KS-Kąkolówka II
GIUS 10–3796/O/229	25x8	Sinusoidal	Oligocene - Rupelian	M-KS-Kąkolówka II
GIUS 10–3796/O/230	20x4	Elongated	Oligocene - Rupelian	M-KS-Kąkolówka II
GIUS 10–3796/O/231	27x10	S-shaped	Oligocene - Rupelian	M-KS-Kąkolówka II

GIUS 10–3796/O/232	26x25	Oval	Oligocene - Rupelian	M-KS-Kąkolówka II
GIUS 10–3796/O/233	38x17	Sinusoidal	Oligocene - Rupelian	M-KS-Kąkolówka II
GIUS 10–3796/O/234	23x11	Curved	Oligocene - Rupelian	M-KS-Kąkolówka II
GIUS 10–3796/O/235	17x5	Elongated	Oligocene - Rupelian	M-KS-Kąkolówka II
GIUS 10–3796/O/236	23x12	Irregular	Oligocene - Rupelian	M-KS-Kąkolówka II
GIUS 10–3796/O/237	32x9	Sinusoidal	Oligocene - Rupelian	M-KS-Kąkolówka II
GIUS 10–3796/O/238	35x11	Curved	Oligocene - Rupelian	M-KS-Kąkolówka II
GIUS 10–3796/O/239	39x12	Elongated	Oligocene - Rupelian	M-KS-Kąkolówka II
GIUS 10–3796/O/240	54x10	S-shaped	Oligocene - Rupelian	M-KS-Kąkolówka II
GIUS 10–3796/O/241	13x4	Sinusoidal	Oligocene - Rupelian	M-KS-Kąkolówka II
GIUS 10–3796/O/242	21x7	Curved	Oligocene - Rupelian	M-KS-Kąkolówka II
GIUS 10–3796/O/243	29x14	Elongated	Oligocene - Rupelian	M-KS-Kąkolówka II
GIUS 10–3796/O/244	12x3	Elongated	Oligocene - Rupelian	M-KS-Kąkolówka II
GIUS 10–3796/O/245	36x13	Elongated	Oligocene - Rupelian	M-KS-Kąkolówka II
GIUS 10–3796/O/246	28x11	Irregular	Oligocene - Rupelian	M-KS-Kąkolówka II
GIUS 10–	56x14	Sinusoidal	Oligocene -	M-KS-

3796/O/247			Rupelian	Kąkolówka II
GIUS 10–3796/O/248	13x11	Oval	Oligocene - Rupelian	M-KS-Kąkolówka II
GIUS 10–3796/O/249	22x7	Curved	Oligocene - Rupelian	M-KS-Kąkolówka II
GIUS 10–3796/O/250	29x16	Curved	Oligocene - Rupelian	M-KS-Kąkolówka II
GIUS 10–3796/O/251	17x4	Elongated, Fig. 2h	Oligocene - Rupelian	M-KS-Wola Czudecka
GIUS 10–3796/O/252	39x15	elongated	Oligocene - Rupelian	M-KS-Wola Czudecka
GIUS 10–3796/O/253	13x3	Elongated, Fig. 2i	Oligocene - Rupelian	M-KS-Wola Czudecka
GIUS 10–3796/O/254	19x4	S-shaped	Oligocene - Rupelian	M-KS-Wola Czudecka
GIUS 10–3796/O/255	28x10	Sinusoidal	Oligocene - Rupelian	M-KS-Wola Czudecka
GIUS 10–3796/O/256	33x15	Irregular	Oligocene - Rupelian	M-KS-Wola Czudecka
GIUS 10–3796/O/257	37x8	S-shaped	Oligocene - Rupelian	M-KS-Wola Czudecka
GIUS 10–3796/O/258	39x11	Curved	Oligocene - Rupelian	M-KS-Wola Czudecka
GIUS 10–3796/O/259	10x4	Elongated, Fig. 2j	Oligocene - Rupelian	M-KS-Wola Czudecka
GIUS 10–3796/O/260	39x9	Elongated	Oligocene - Rupelian	M-KS-Wola Czudecka
GIUS 10–3796/O/261	36x13	Sinusoidal	Oligocene - Rupelian	M-KS-Wola Czudecka
GIUS 10–3796/O/262	24x24	Oval	Oligocene - Rupelian	M-KS-Wola Czudecka
GIUS 10–3796/O/263	15x7	Curved	Oligocene - Rupelian	M-KS-Wola Czudecka
GIUS 10–3796/O/264	26x5	Sinusoidal	Oligocene - Rupelian	M-KS-Wola Czudecka
GIUS 10–3796/O/265	33x14	Irregular	Oligocene - Rupelian	M-KS-Wola Czudecka
GIUS 10–3796/O/266	14x4	Curved	Oligocene - Rupelian	M-KS-Wola Czudecka
GIUS 10–3796/O/267	36x13	Sinusoidal	Oligocene - Rupelian	M-KS-Wola Czudecka
GIUS 10–	38x11	Elongated	Oligocene -	M-KS-Wola

3796/O/268			Rupelian	Czudecka
GIUS 10–3796/O/269	50x22	S-shaped	Oligocene - Rupelian	M-KS-Wola Czudecka
GIUS 10–3796/O/270	12x13	Sinusoidal	Oligocene - Rupelian	M-KS-Wola Czudecka
GIUS 10–3796/O/271	28x7	Elongated	Oligocene - Rupelian	M-KS-Wola Czudecka
GIUS 10–3796/O/272	35x14	Curved	Oligocene - Rupelian	M-KS-Wola Czudecka
GIUS 10–3796/O/273	21x18	Oval	Oligocene - Rupelian	M-KS-Wola Czudecka
GIUS 10–3796/O/274	20x4	Elongated, Fig. 2k	Oligocene - Rupelian	M-KS-Wola Czudecka
GIUS 10–3796/O/275	42x16	Elongated	Oligocene - Rupelian	M-KS-Wola Czudecka
GIUS 10–3796/O/276	38x5	Sinusoidal	Oligocene - Rupelian	M-KS-Wola Czudecka
GIUS 10–3796/O/277	39x9	S-shaped	Oligocene - Rupelian	M-KS-Wola Czudecka
GIUS 10–3796/O/278	41x13	Sinusoidal	Oligocene - Rupelian	M-KS-Futoma
GIUS 10–3796/O/279	11x9	Oval, Fig. 2l	Oligocene - Rupelian	M-KS-Futoma
GIUS 10–3796/O/280	11x4	Elongated	Oligocene - Rupelian	M-KS-Futoma
GIUS 10–3796/O/281	19x6	S-shaped	Oligocene - Rupelian	M-KS-Futoma
GIUS 10–3796/O/282	9x4	Irregular, Fig. 2m	Oligocene - Rupelian	M-KS-Futoma
GIUS 10–3796/O/283	33x9	Sinusoidal	Oligocene - Rupelian	M-KS-Futoma
GIUS 10–3796/O/284	35x11	Curved	Oligocene - Rupelian	M-KS-Futoma
GIUS 10–3796/O/285	32x13	Elongated	Oligocene - Rupelian	M-KS-Wujskie
GIUS 10–3796/O/286	20x7	Sinusoidal	Oligocene - Rupelian	M-KS-Wujskie
GIUS 10–3796/O/287	26x5	Sinusoidal	Oligocene - Rupelian	M-KS-Wujskie
GIUS 10–3796/O/288	11x3	Elongated	Oligocene - Rupelian	M-KS-Wujskie
GIUS 10–3796/O/289	19x4	Elongated	Oligocene - Rupelian	M-KS-Rudawka Rymanowska
GIUS 10–	45x15	Sinusoidal	Oligocene -	M-KS-

3796/O/290			Rupelian	Rudawska Rymanowsk a
GIUS 10–3796/O/291	28x15	Sinusoidal	Oligocene - Rupelian	M-KS-Rudawka Rymanowsk a
GIUS 10–3796/O/292	14x11	Oval	Oligocene - Rupelian	M-KS-Jamna Dolna
GIUS 10–3796/O/293	57x10	Curved	Oligocene - Rupelian	M-KS-Jamna Dolna
GIUS 10–3796/O/294	10x4	Elongated, Fig. 2t	Oligocene - Rupelian	M-KS-Jamna Dolna
GIUS 10–3796/O/295	19x13	Irregular	Oligocene - Rupelian	M-KS-Jamna Dolna
GIUS 10–3796/O/296	22x7	Elongated	Oligocene - Rupelian	M-KS-Jamna Dolna
GIUS 10–3796/O/297	9x7	Oval, Fig. 3a	Oligocene - Rupelian	M-KS-Równe
GIUS 10–3796/O/298	13x13	Oval	Oligocene - Rupelian	M-KS-Równe
GIUS 10–3796/O/299	54x6	Sinusoidal, Fig.3b	Oligocene - Rupelian	M-KS-Jasienica Rosielna
GIUS 10–3796/O/300	20x4	Curved	Oligocene - Rupelian	M-KS-Jasienica Rosielna

Table 2 (on next page)

Miocene coprolite list.

Table 2:

Miocene coprolite list.

Specimen	Dimensions (mm)	Shape	Age	Site
GIUS 10–3796/M/1	36x28	Oval	Miocene - Langhian	Kleszczów Graben area-Bełchatów
GIUS 10–3796/M/2	25x15	Irregular, Fig. 3l	Miocene - Langhian	Kleszczów Graben area-Bełchatów
GIUS 10–3796/M/3	19x17	Oval	Miocene - Langhian	Kleszczów Graben area-Bełchatów
GIUS 10–3796/M/4	21x17	Oval	Miocene - Langhian	Kleszczów Graben area-Bełchatów
GIUS 10–3796/M/5	27x8	Curved	Miocene - Langhian	Kleszczów Graben area-Bełchatów
GIUS 10–3796/M/6	20x10	Elongated, Fig. 3m	Miocene - Langhian	Kleszczów Graben area-Bełchatów
GIUS 10–3796/M/6(1)	18x8	Elongated	Miocene - Langhian	Kleszczów Graben area-Bełchatów
GIUS 10–3796/M/6(2)	16x10	Elongated	Miocene - Langhian	Kleszczów Graben area-Bełchatów
GIUS 10–3796/M/6(3)	19x11	Elongated	Miocene - Langhian	Kleszczów Graben area-Bełchatów
GIUS 10–3796/M/6(4)	15x8	Elongated	Miocene - Langhian	Kleszczów Graben area-Bełchatów
GIUS 10–3796/M/6(5)	19x12	Elongated	Miocene - Langhian	Kleszczów Graben area-Bełchatów
GIUS 10–3796/M/7	27x25	Oval	Miocene - Langhian	Kleszczów Graben area-Bełchatów
GIUS 10–3796/M/8	37x13	Elongated	Miocene - Langhian	Kleszczów Graben area-Bełchatów
GIUS 10–	47x18	Irregular	Miocene -	Kleszczów

3796/M/9			Langhian	Graben area-Bełchatów
GIUS 10–3796/M/10	31x30	Oval	Miocene - Langhian	Kleszczów Graben area-Bełchatów
GIUS 10–3796/M/11	25x20	Oval, Fig. 3n	Miocene - Langhian	Kleszczów Graben area-Bełchatów
GIUS 10–3796/M/12	16x5	Sinusoidal	Miocene - Langhian	Kleszczów Graben area-Bełchatów
GIUS 10–3796/M/13	20x8	Elongated, Fig. 3e	Miocene - Langhian	Gołuchów quarry
GIUS 10–3796/M/14	40x14	S-shaped	Miocene - Burdigalian	Turów area
GIUS 10–3796/M/15	61x24	Curved	Miocene - Burdigalian	Turów area
GIUS 10–3796/M/16	50x20	Elongated, Fig. 3g	Miocene - Burdigalian	Turów area
GIUS 10–3796/M/17	34x24	Oval	Miocene - Burdigalian	Turów area
GIUS 10–3796/M/18	41x13	S-shaped	Miocene - Burdigalian	Turów area
GIUS 10–3796/M/19	55x17	Curved, Fig. 3h	Miocene - Burdigalian	Turów area
GIUS 10–3796/M/20	36x18	Elongated	Miocene - Burdigalian	Turów area
GIUS 10–3796/M/21	40x14	Sinusoidal	Miocene - Burdigalian	Turów area
GIUS 10–3796/M/22	31x10	S-shaped	Miocene - Burdigalian	Turów area
GIUS 10–3796/M/23	62x31	Irregular, Fig. 3i	Miocene - Burdigalian	Turów area
GIUS 10–3796/M/24	54x23	Sinusoidal	Miocene - Burdigalian	Turów area
GIUS 10–3796/M/25	36x16	Sinusoidal	Miocene - Burdigalian	Turów area
GIUS 10–3796/M/26	30x30	Oval	Miocene - Burdigalian	Turów area
GIUS 10–3796/M/27	48x19	Elongated	Miocene - Burdigalian	Turów area
GIUS 10–3796/M/28	78x20	Curved, Fig.3j	Miocene - Burdigalian	Turów area
GIUS 10–3796/M/29	73x25	Elongated	Miocene - Burdigalian	Turów area
GIUS 10–	66x27	S-shaped,	Miocene -	Turów area

3796/M/20		Fig. 3k	Burdigalian	
GIUS 10–3796/M/31	41x13	Curved	Miocene - Burdigalian	Turów area
GIUS 10–3796/M/32	33*14	Elongated, Fig. 3f	Miocene - Serravalian	Roztocze area-Żelebsko
GIUS 10–3796/M/33	23x5	Elongated, Fig. 3d	Miocene - Burdigalian	M-KS-Temeszów
GIUS 10–3796/M/34	30x10	Elogated	Miocene - Burdigalian	M-KS-Brzuska

4

Table 3(on next page)

Oligocene localities with coprolites and their morphologies.

Table 3:
Oligocene localities with coprolites and their morphologies.

	SHAPE						
Locality	**Sinusoidal**	**Elongated**	**Oval**	**More or less regular**	**S-shaped**	**Curved**	**Summary**
M-KS-Kąkolówka I	40	23	18	17	22	30	150
M-KS-Kąkolówka II	34	21	8	7	17	13	100
M-KS-Wola Czudecka	6	9	2	1	4	5	27
M-KS-Futoma	2	1	1	1	1	1	7
M-KS-Jamna Dolna	-	2	1	1	-	1	5
M-KS-Rudawka Rymanowska	2	1	-	-	-	-	3
M-KS-Równe	-	-	2	-	-	-	2
M-KS-Wujskie	2	2	-	-	-	-	4
M-KS-Jasienica Rosielna	1	-	-	-	-	1	2

Table 4(on next page)

Miocene localities with coprolites and their morphologies.

Table 4:

Miocene localities with coprolitesand their morphologies.

	SHAPE						
Locality	**Sinusoidal**	**Elongated**	**Oval**	**More or less regular**	**S-shaped**	**Curved**	**Summary**
Kleszczów Graben area	5	9	2	1	-	1	17
Turów area	3	4	2	1	4	4	18
Gołuchów quarry	-	1	-	-	-	-	1
Roztocze area-Żelebsko							1
M-KS-Temeszów	-	1	-	-	-	-	1
M-KS-Brzuska	-	1	-	-	-	-	1